



**Manuel Joaquim dos Santos Moreira da Silva**

Bachelor's Degree in sciences of Physics Engineering

## **Optimization and Automation of the Nuclear Reaction Chamber**

Dissertation submitted in partial fulfillment  
of the requirements for the degree of Physics Engineering

Master of Science in  
**Physics Engineering**

Adviser: Prof. Dr. Micaela Fonseca, Invited Assistant Professor  
NOVA University of Lisbon

Co-Advisor: Prof. Dr. João Cruz, Associate Professor  
NOVA University of Lisbon

Examination Committee:

Chair: Prof. Dr. André Wemans,  
NOVA University of Lisbon

Members: Prof. Dr. Micaela Fonseca, Invited assistant  
professor  
NOVA University of Lisbon

Prof. Dr. Orlando Teodoro  
NOVA University of Lisbon



FACULDADE DE  
CIÊNCIAS E TECNOLOGIA  
UNIVERSIDADE NOVA DE LISBOA

**Dezembro, 2020**





## **Optimization of the Tandem Accelerator**

Copyright © Manuel Joaquim dos Santos Moreira da Silva, Faculty of Sciences and Technology, NOVA University Lisbon. The Faculty of Sciences and Technology and the NOVA University Lisbon have the right, perpetual and without geographical boundaries, to file and publish this dissertation through printed copies reproduced on paper or on digital form, or by any other means known or that may be invented, and to disseminate through scientific repositories and admit its copying and distribution for non-commercial, educational or research purposes, as long as credit is given to the author and editor.

*Life is strong and fragile. It's a paradox... It's both things, like quantum physics:  
It's a particle and a wave at the same time. It all exists all together.*  
*Joan Jett*



## **Acknowledgements**

Antes de mais gostava de agradecer aos meus pais. Este trabalho é-lhes dedicado com especial carinho para ambos, à minha mãe por me mostrar a bondade nas pessoas e ao meu pai por nunca duvidar de mim e me encorajar quando mais precisava. E ambos em conjunto por me mostrarem como amar.

Aos meus orientadores, a Micaela Fonseca por ter paciência comigo e fazer horas extraordinárias para que este trabalho fosse concluído a tempo, e ao professor João Cruz pelo excelente humor e por se disponibilizar sempre que precisava de ajuda.

Ao Doutor Rodrigo Mateus pela ajuda na gaiola e desenhos para a tampa na câmara de vácuo.

Ao Faustino por toda a ajuda que me deu na construção da gaiola de faraday assim como na assistência na parte técnica da construção.

Ao André Fernandes por toda a amizade que me deu durante a minha carreira académica.

To my beloved Wiczán that showed me a whole new world of adventure and fun.

A todos os que direta ou indiretamente me ajudaram com o projeto.





# Abstract

---

The production of vacuum is usually a very lengthy process that occupies precious research time. When dealing with many samples, the amount of times vacuum will have to be produced is directly tied to the number of samples a sample holder can take. This problem becomes much more important when dealing with samples that take longer to generate vacuum in the vacuum chamber, such as biological samples.

Associated with this work is the construction of a new sample holder capable of holding up to fifteen samples, a new lid associated with the necessities of the new design, the incorporation of a linear feedthrough and a rotary platform, the construction of a new faraday cage to minimize associated noise and coding to automatically alternate between samples in both a linear and angular fashion. This new setup is going to be mounted in the target chamber of the nuclear reactions beam line of the 3.0 MV tandem accelerator located at CTN-IST (Bobadela Campus) and will give the nuclear reactions group new analysis capabilities.

The design of the new parts was done with the usage of SolidWorks, and the development of the code was done with the usage of both Python for the user interface and Arduino for the control of the motors motion.

**Keywords:** 3D modelling, Sample holder, Faraday cage, vacuum devices, nuclear reactions.



# Resumo

---

A produção de vácuo tende a ser um processo muito demoroso interferindo negativamente com a investigação. Quando se lida com um elevado número de amostras, o número de vezes que vácuo tem de ser produzido está diretamente associado ao número de amostras que um determinado porta-amostras consegue suportar. Este problema torna-se mais notório quando nos deparamos com amostras que tendem a levar mais tempo a gerar vácuo como é o caso de amostras biológicas.

Associado a este trabalho está a construção de um novo porta-amostras com capacidade para suportar quinze amostras, uma nova tampa para a câmara de vácuo associada às necessidades do novo design, a incorporação de um feedthrough linear e uma plataforma rotativa, a construção de uma nova gaiola de Faraday para minimizar o ruído eletrónico nos detetores de radiação e a escrita de código para controlar remotamente o posicionamento das amostras (translação e rotação). Esta nova configuração ficará operacional na câmara de alvos da linha de reações nucleares do acelerador tandem de 3,0 MV localizado no CTN-IST (Campus da Bobadela) e dará ao grupo de reações nucleares novas capacidades de análise.

O design das novas peças foi feito com o uso do SolidWorks e o desenvolvimento do código foi feito com o uso do Python para a interface do usuário e do Arduino para o controlo do movimento dos motores ligados ao novo porta-amostras.

Palavras Chave: Modelação 3D, Porta-amostras, Gaiola de Faraday, Sistemas de Vácuo, reações nucleares.

---





# Contents

1	Introduction .....	1
1.1	Motivation .....	1
1.2	Objectives .....	2
1.3	State of the art .....	2
1.4	Structure of the thesis.....	2
2	Theoretical Background .....	4
2.1	Nuclear Reactions.....	5
2.1.1	Elastic scattering.....	5
2.2	Cross Section .....	8
2.3	Stopping power .....	9
2.4	Stepper motors.....	10
2.5	Analyses methods in the vacuum chamber.....	13
2.5.1	PIGE.....	13
2.5.2	Nuclear Reaction Analysis .....	15
2.5.3	Rutherford Backscattering Spectroscopy .....	17
2.6	Faraday Cage .....	18
3	Equipment, Materials and Methods .....	19
3.1	Present parts .....	20
3.1.1	Tandem accelerator.....	20
3.1.1.1	Duoplasmatron ion source .....	21
3.1.1.2	Beam transport chamber .....	23
3.1.1.3	Nuclear Reaction Chamber.....	24
3.1.1.4	Stripping.....	26
3.2	Acquired parts.....	27
3.2.1	Faraday Cage .....	27
3.2.2	Sample Holder .....	31
3.2.2.1	Sample holder past designs .....	34
3.2.3	Sample holder motion .....	36

3.2.3.1	Angular Motion .....	37
3.2.3.2	Linear Motion.....	39
3.2.4	New Lid.....	41
4	Code structure .....	43
4.1	Graphical User Interface.....	44
4.2	Standard Mode .....	44
4.3	Manual mode .....	47
4.4	System connections.....	50
4.4.1	Python to Arduino to Gecko drive to Motors .....	50
5	Summary and Final Remarks.....	53
5.1	Conclusions .....	53
5.2	Future Prospects .....	54
6	References .....	55
7	Appendix.....	59
7.1	Code .....	59
7.1.1	Python.....	59
7.1.1.1	Arduino.....	68
7.2	Blueprints .....	71
7.2.1	Faraday Cage .....	71
7.2.2	Sample Holder.....	73
7.2.3	Lid.....	75
7.2.4	Isolating Piece .....	76
7.2.5	Connecting Rod .....	77

# List of Figures

Figure 2.1- Schematic view of the time evolution of a nuclear reaction .....	5
Figure 2.2- Representation of the Rutherford Scattering Experiment conducted by Rutherford in 1911 .....	6
Figure 2.3 - Elastic collision of a neutron and a Uranium 238 nucleus .....	7
Figure 2.4 - Schematic of the cross section.....	8
Figure 2.5 - Variable-reluctance stepper motor.....	11
Figure 2.6 - Stepper motor characteristics .....	12
Figure 2.7 - Figure 2.7 PIGE spectrum of an archaeological sample (obsidian glass) (left) and PIGE spectrum of an aerosol sample) (right).....	14
Figure 2.8 - Collision of a $^3\text{He}$ with a $^2\text{H}$ resulting in a $^4\text{He}$ and a $^1\text{H}$ .....	16
Figure 2.9 - Cross Section for the $^{18}\text{O}(p, \alpha)^{15}\text{N}$ reaction at $165^\circ$ .....	16
Figure 2.10 - Example of a RBS experiment.....	17
Figure 2.11 - Visual experimentation of RBS.....	18
Figure 2.12 - Visual representation of the reorganization of the charges of the cage's walls in response to an exterior field.....	18
Figure 3.1 - CTN tandem accelerator .....	20
Figure 3.2 - Labeled Schematic of an Duoplasmatron ion source .....	22
Figure 3.3 –Diagram of the nuclear reaction line of the tandem accelerator, adapted from [3]. .....	22
Figure 3.5 - Labeled Schematic of an Duoplasmatron ion source .....	23
Figure 3.6 - Labeled internal image of a tandem accelerator [23].....	24



Figure 3.7 – Cross section of the stripping chamber .....	25
Figure 3.8 - Photo of the nickel plate that protects the nuclear reaction chamber without the inclusion of the golden plate(left) and photo of the nickel plate that protects the nuclear reaction chamber with the inclusion of the golden plate(right). Taken from [1])......	26
Figure 3.9 - Photo of the interior of the nuclear reaction chamber with the referred parts. [1].....	26
Figure 3.10- Electrical isolation of the Faraday Cage. ....	28
Figure 3.11 - Labeled representation of the new Faraday Cage (right) and non-labeled version of the cage (left). ....	29
Figure 3.12 - Installed Faraday Cage. ....	30
Figure 3.11 - Labeled representation of the sample holder. ....	31
Figure 3.12 - Removable C shaped edge .....	32
Figure 3.13 - Example of a laminal sample holder inserted .....	33
Figure 3.14 - Connection vein attached to isolation area .....	33
Figure 3.15 - Sample holder's first design .....	34
Figure 3.16 - Sample holder's second design.....	35
Figure 3.17 - Sample holder's third design .....	36
Figure 3.18 - Design presented by the workshops.....	37
Figure 3.19 - Labeled Rotary platform.....	37
Figure 3.20 - Cross section of the Rotary Platform .....	39
Figure 3.21 - Labeled Feedthrough .....	40
Figure 3.22 - Connection to the rod stated in chapter 3.2.2 .....	41
Figure 3.23 - Representation of both parts properly attached to one another, from the side represented on the left, and from the top represented on the right .	41
Figure 3.24 - 3D modeling of the new Lid.....	42
Figure 3.25 - Typical BNC connector .....	43

Figure 4.1- Initial menu to choose between two modes.....	45
Figure 4.2 - User GUI of the program.....	46
Figure 4.3(a) - Flowchart of the program for Next Sample .....	47
Figure 4.3(b) - Flowchart of the program for Previous Sample .....	47
Figure 4.4 -Initial display of the program .....	48
Figure 4.5 - Secondary Display with 5 samples selected in the first display	49
Figure 4.6: - Labeled version of Figure 4.5 .....	50
Figure 4.7 - Positioning considered by the program of vertical positions (left) and angular positions (right) as displayed in Figure 4.8.....	50
Figure 4.8 - Example of a filled UI (left) and first position of the sample (right) .....	51
Figure 4.9 - Gecko connections .....	52



# Acronyms

IBA	Ion beam analysis
PIGE	Proton-Induced Gamma-ray Emission
CTN	Centro Tecnológico e Nuclear
ICRU Measurements	International Commission on Radiation Units and Measurements
DC	Direct Current
PM	Permanent Magnet
PIGE	Particle Induced X-ray Emission
NRA	Nuclear Reaction Analysis
RBS	Rutherford backscattering spectrometry
BNC	Bayonet Neill Concelman (connector)
GUI	Graphical User Interface
UI	User Interface





## Introduction

### 1.1 Motivation

As of recent years, the usage of Ion Beam Analysis (IBA) has become an important group of analytical techniques that are widely used in applications ranging from analysis of fission reactor material to biomedicine, environment, cultural heritage, and more recently, fusion reactor technologies.

The technique uses energetic ion beams to probe the surface of materials. The IBA techniques are non-destructive, highly sensitive ( $\text{pg/g}$  range) and allow the detection of elements in depths ranging up to several tenths of micrometers.

Amongst the various IBA techniques, PIGE or Particle-Induced Gamma-ray Emission will be the one being focused on this thesis. PIGE involves the measurement of the energy of the gamma rays emitted by a certain sample when bombarded with charged particles.

This leads us to the current obstacle that the Nuclear Reactions Group involved in PIGE measurements is facing. When dealing with many samples, the process of changing samples positioned in vacuum inside the target chamber becomes very time consuming. The current sample holder can only take up to 4 samples at a time. When the group members are involved in studying large sample batches, a significant amount of time is lost in the operation of refilling the sample holder since high vacuum must be set before putting the beam on.

# Chapter 1: Introduction

---

## 1.2 Objectives

The main objective of this thesis is to solve the problem that was presented in the motivation.

To achieve this, the following sub goals needed to be achieved.

- Design, construction of a new sample holder that can hold 15 samples.
- Development of code that interfaces the user with the sample holder's vertical and angular position, thus allowing to switch between samples to be irradiated by the beam.
- Construction of a new Faraday Cage.
- Construction of a lid to support the whole system.

## 1.3 State of the art

The former sample holder used by the nuclear reactions group had space for only four samples and functioned in a one-dimensional system, it could either go up or down [1]. Plus, this sample holder had to be operated manually.

Also, research utilizing the previous setup were facing a recurring charge collection issues due to electronic noise problems [3].

To avoid this problem a new faraday cage construction started as part of Kateline Dias thesis work [2] and was concluded in this work.

## 1.4 Structure of the thesis

This thesis is divided into a total of five chapters. In chapter two the theoretical background is presented, including an introduction to the nuclear reactions of interest, and some of the analyses conducted by the nuclear reactions group. It ends by describing the necessity of the development of this thesis.

Chapter 3 is divided into three segments. The first describes the present equipment at CTN (Centro Tecnológico e Nuclear – IST). The second gives an in-depth description of the design, construction, and installation of the newly constructed material, which includes the faraday cage, the new sample holder

# Chapter 1: Introduction

---

and the new lid. The third segment gives a discussion of the LewVac linear feedthrough and the Two Stage Differentially Pumped Rotary Platform.

Chapter 4 explains the logic behind the code in both Arduino and Python that was written for this work, the connection from the python system into the Arduino system into the actual motorized system.

Finally, chapter 5 summarizes the work done throughout this master thesis and subsequent prospects.



CHAPTER 2

## Theoretical Background

To contextualize the work carried out within the scope of this thesis in the investigation conducted by the nuclear reactions group, a theoretical background on relevant topics will be discussed in this chapter. It details the theory behind the nuclear reactions as a whole and in particular the topics cross section and stopping power. A brief explanation of some of the analysis methods that have been performed by the group will also be presented. This chapter is important for the comprehension of the methodology used in the experiments conducted in the Tandem Accelerator. Other aspects more directly related to the work conducted will also be discussed, aspects like the basis of a Faraday Cage and of stepper motors.

# Chapter 2: Theoretical Background

## 2.1 Nuclear Reactions

In the year of 1919, Ernest Rutherford and his team produced for the first time a nuclear reaction at the University of Manchester [4]. The experiment consisted in colliding alpha particles with Nitrogen creating Oxygen. Chemical reactions usually take place when electrons interact with one another, nuclear reactions, like chemical reactions, take place by a variety of reaction mechanisms [5]. Below a simple model is presented for the typical nuclear reaction divided into three stages.

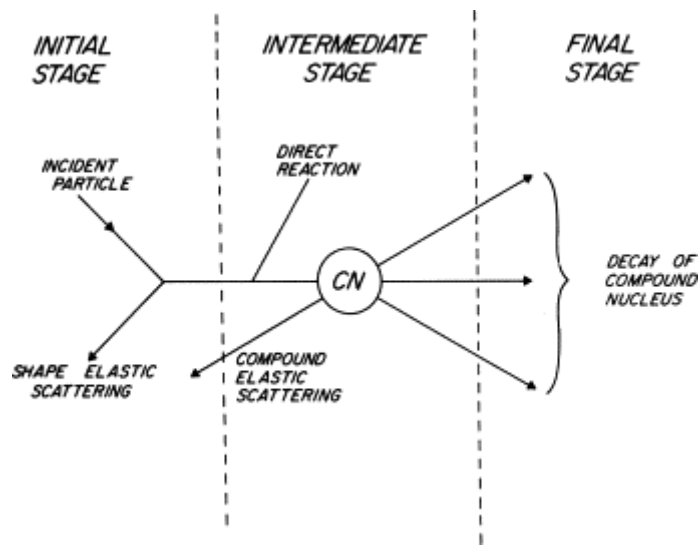


Fig. 2.1 - Schematic view of the time evolution of a nuclear reaction [25].

The element may penetrate the nucleus entirely resulting in the disruption of the nucleons or be dispersed by the nucleus field. In the subchapters below some of the main types of nuclear reactions will be explored, those of elastic and inelastic scattering and transfer reactions.

### 2.1.1 Elastic scattering

The basis of Elastic Scattering is the conservation of the total kinetic energy of the system.

A good example of Elastic Scattering in Nuclear physics is the case of Rutherford Scattering, explained by Ernest Rutherford. In Rutherford Scattering a high energy charged particle (for example an alpha particle or an electron) interacts with a nucleus and is scattered via Colombian force. These scattered particles can be found in large deflection angles and can even be found to be

## Chapter 2: Theoretical Background

backscattered. This experiment was essential to the construction of the Rutherford model of the atom.

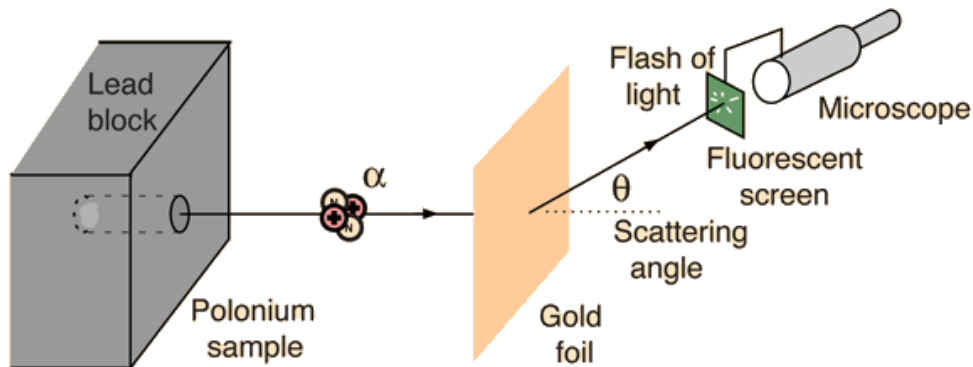
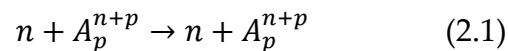


**Fig 2.2 - Representation of the Rutherford Scattering Experiment conducted by Rutherford in 1911 [26].**

Elastic scattering is the principal mode of interaction of neutrons ( $n$ ) with atomic nuclei ( $A$ ) [7]. In this process, the target nucleus remains in the same state after interaction, in terms of nomenclature, the description of these reactions can be written as  $A(n, n)A$ , or in a more detailed way, like so



Elastic scattering can be described in two modes, potential and resonant, in potential elastic scattering the neutron is acted by the short-range nuclear forces, and thus simply scatters off it without colliding with the nucleus. In the resonance case, if the neutron has the correct amount of energy, the nucleus absorbs the neutron and emits a neutron with the same energy, this can be seen in the graph below [8]

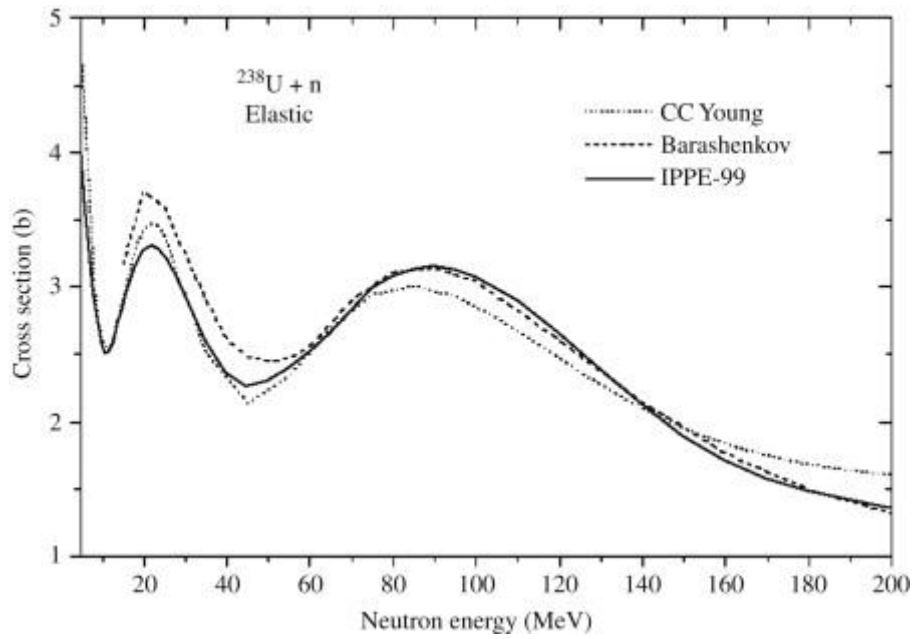


**Fig. 2.3 - Elastic collision of a neutron and a Uranium 238 nucleus [8].**

The resonant energies of the uranium atom in the graph are represented by the different peaks in the colliding neutron energy.

# Chapter 2: Theoretical Background

## 2.2 Cross Section

Cross section of a nucleus can be described as the probability that a certain nuclear reaction will occur, this concept can be conceptualized physically with an area, the larger the area, the higher the probability. The standard unit of measurement of the cross section is the barn (represented with a  $\sigma$ ), equating to an area of  $10^{-28}\text{m}^2$ . Let's consider a detector that will detect particles in a nuclear reaction, this reaction will emit particles in the direction of  $(\theta, \phi)$ , in relation to the beam directed to the sample being analyzed with an intensity of  $I_\alpha$ .

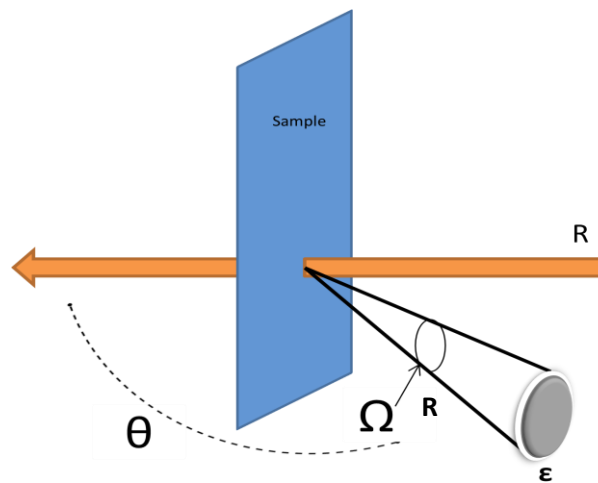


**Fig 2.4 - Schematic of the cross section, where  $\theta$  is the scattering angle,  $\Omega$  is the solid angle,  $\epsilon$  is the efficiency of the detector and  $R$  is the rate at which the particles are produced.**

In this situation, the cross section  $\sigma$  can be determined by the equation, where  $I_\alpha$  represents the intensity of the colliding beam and  $Nt$  represents the number of particles at a certain time interval and  $R_b$  the rate that the particles are produced. [25]:

$$d\sigma = \frac{dR_b}{I_\alpha N_t} \quad (2.2)$$

## Chapter 2: Theoretical Background

---

Above we have a representation of a detector. Due to its limited solid angle, this detector only acquires a fraction of the particles produced in the nuclear reaction.

These particles usually are not emitted isotropically, and follow a distribution pattern  $r$  that depends on the values of  $\theta$  and  $\phi$ . With this in mind, we can write the equation as [25]:

$$d\sigma = r(\theta, \phi) \frac{d\Omega}{4\pi} \quad (2.3)$$

where  $d\Omega/4\pi$  gives the fraction of solid angle covered by the detector and  $r(\theta, \phi)$  represents the angular distribution of particles.

With the equations 2.1 and 2.2 we can arrive at the equation [25]:

$$\frac{d\sigma}{d\Omega} = \frac{r(\theta, \phi)}{4\pi I_a N_t} \quad (2.4)$$

Integrating this result in all angles, and over a spherical area, we can arrive at the final equation (considering  $d\sigma = \sin(\theta)d(\theta)d(\phi)$ ) [25]:

$$\sigma = \int_{d\Omega} \frac{d\sigma}{d\Omega} d\Omega = \int_0^\pi \sin(\theta) d\theta \int_\pi^{2\pi} d\phi \frac{d\sigma}{d\Omega} \quad (2.5)$$

# Chapter 2: Theoretical Background

---

## 2.3 Stopping power

The International Commission on Radiation Units and Measurements or ICRU defined the physical quantity stopping power [12] as the average energy dissipated by ionizing radiation in a medium per unit path length of travel of the radiation in the medium. Or in other words we can describe it as a retarding force acting on charged particles, when they interact with matter, this results in a loss of energy of the particle [13].

Although impossible to predict the individual loss of energy of an atom going through an absorber medium, the average becomes possible when taking into account the charge, mass and energy of the particle, as well as the atomic number ( $Z$ ) and the density of the absorbing medium. Bethe [14] derived the equation to calculate the stopping power that comes from Coulombian forces of heavy charged particles (e.g., alpha particles, protons, and deuterons) traveling through the absorbing medium.

Later, in 1984 Rohrlich and Carlson [15] refined the equation to include energy losses via bremsstrahlung radiation, significant when high-energy electrons and beta particles interact with absorbers of high atomic number. The equation can be presented ahead [15].

$$\frac{dE}{dx} = 4 \frac{\pi r_0^2 m c^2}{\beta^2} N Z \left[ \ln \left( \frac{2 m c^2}{E} \beta^2 \gamma^2 \right) - \beta^2 \right] \quad (2.6)$$

Where  $dE/dx$  is the particle stopping power in units of MeV/m,  $r_0$  is the classical electron radius =  $2.818 \times 10^{-15}$  m,  $z$  is the charge on the particle ( $z = 1$  for p, d,  $\beta^-$ ,  $\beta^+$  and  $z = 2$  for  $\alpha$ ),  $m c^2$  is the rest energy of the electron = 0.511 MeV,  $N$  is the number of atoms per  $m^3$  in the absorber material through which the charged particle travels ( $N = \rho(N_A/A)$  where  $\rho$  is the absorber density (e.g., for NaI,  $\rho = 3.67 \text{ g.cm}^{-3}$ ),  $N_A$  is Avogadro's number =  $6.022 \times 10^{23}$  atoms per mol,  $A$  and  $Z$  are the atomic weight and atomic number, respectively, of the absorber.

# Chapter 2: Theoretical Background

---

## 2.4 Stepper motors

A stepper motor is a device that converts DC voltage into mechanical rotation of its shaft. The motor functions both as an actuator and as a position transducer. The discrete motion of motor makes it perfectly suited to utilize it with digitally based control systems such as an Arduino since its motion is directly tied to individual steps [16].

The speed of a stepper motor can be changed by altering the rate of the pulse input, for example, a stepper motor that would require 48 pulses to rotate a full revolution, an input of 96 pulses per second would rotate the equivalent of twice the usual speed, be that 120 rev/min. The rotation of the motor is actually done in very small increments; however, these increments are visually indiscernible at all but the lowest speeds.

Some stepper motors are capable of sustaining a 2.2 kW load with stepping rates from 1000 to 20 000 per second in angular increments from 45° down to 0.75°, these small angular increments can be extremely useful when conducting very precise movement experiments.



## Chapter 2: Theoretical Background

There are three basic types of stepper motor:

- **Variable reluctance:** With a wound stator, this type of stepper motor possesses a soft iron multi-toothed rotor. With the winding configuration and excitation, the number of teeth on the stator and rotor is what ends up defining the value of the angle per step. This type of stepper motor operates at high step rates and gives us a small to medium-sized step angles when compared to its counterparts.
- **Permanent magnet:** The type of rotor utilized in the permanent magnet type of stepper motor consists of a cylindrical permanent magnet that is fixed in the shaft. Permanent Magnet stepper motors provide a fairly large step angle, ranging from  $45^\circ$  all the way up to  $120^\circ$ .
- **Hybrid:** The hybrid stepper motor is a combination of both the PM-motor and the VR-motor. Usually, the stator has eight salient poles which are energized by a two-phase winding. The rotor consists of a cylindrical magnet which is magnetized along its axis. The step angle depends on the method of construction and is generally in the range  $0.9\text{-}5^\circ$ .

In Fig 2.5 the basic principle of operation of a stepper motor is shown. This stepper motor as a total of eight stator teeth (displayed in proximity to the stator), and six rotor teeth (presented on top of the rotor)

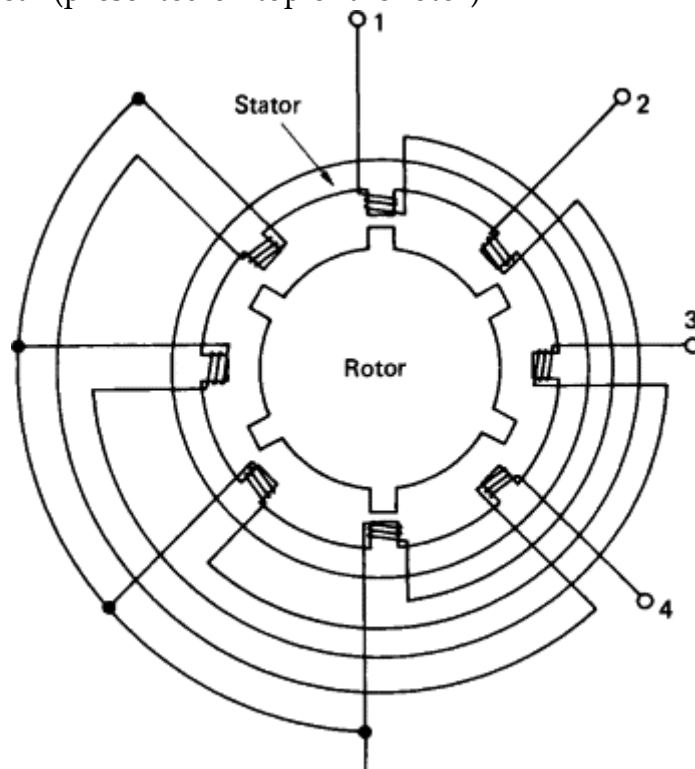


Figure 2.5 - Variable-reluctance stepper motor [16].

## Chapter 2: Theoretical Background

If phase 1 of the stator is activated on its own, 2 diametrically opposed rotor teeth align themselves with the phase 1 teeth of the stator. After this, the next set of rotor teeth adjacent to the first one is then  $15^\circ$  out of step with those of the stator. Activation of the phase 2 winding on its own would cause the rotor to rotate again a total of  $15^\circ$  in the anti-clockwise direction to align the adjacent pair of diametrically opposite rotor teeth. If the stator windings are excited in the sequence 1, 2, 3, 4 the rotor will move in consecutive  $15^\circ$  steps in the anti-clockwise direction.

The general characteristics of a typical stepper motor are given in Fig. 2.7. When a pulse is applied, and with each sequential pulse the rotor of the stepper motor will quickly accelerate towards a new step position. Without the usage sufficient retarding force there could be some overshoot and oscillation. These oscillations can cause rotor resonance at certain pulse frequencies, resulting in loss of torque, or in a worst-case scenario pull-out condition. As variable-reluctance motors have very little inherent damping, they are more susceptible to resonances than either the hybrid types or the permanent magnet. Mechanical and electronic dampers are available which can be used to minimize the adverse effects of rotor resonance. If possible, however, the motor should be selected such that its resonant frequencies are not critical to the application under consideration [16].

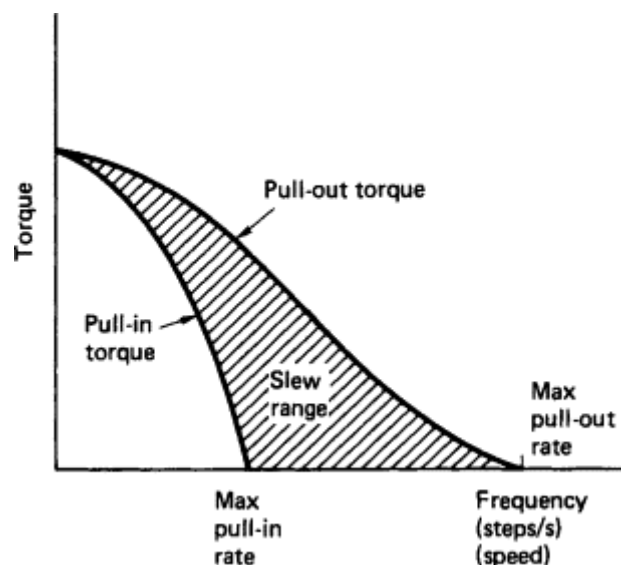


Figure 2.6 - Stepper motor characteristics [16].

# Chapter 2: Theoretical Background

---

Bellow some of the basic terms regarding stepper motors are presented.

- *Pull-out torque*: The maximum torque which can be applied to a motor, running at a given stepping rate, without losing synchronism.
- *Pull-in torque*: The maximum torque against which a motor will start, at a given pulse rate, and reach synchronism without losing a step.
- *Dynamic torque*: The torque developed by the motor at very slow stepping speeds.
- *Holding torque*: The maximum torque which can be applied to an energized stationary motor without causing spindle rotation.
- *Pull-out rate*: The maximum switching rate at which a motor will remain in synchronism while the switching rate is gradually increased.
- *Pull-in rate*: The maximum switching rate at which a loaded motor can start without losing steps.
- *Slew range*: The range of switching rates between pull-in and pull-out in which a motor will run in synchronism but cannot start or reverse.

## 2.5 Analyses methods in the vacuum chamber

We may now discuss the different types of Nuclear Reaction Analysis that are utilized in the vacuum chamber that will be worked on.

### 2.5.1 PIGE

PIGE stands for Particle-Induced Gamma-ray Emission and is typically used to analyze bulk samples. In this technique, the sample positioned inside a vacuum chamber (or target chamber) is bombarded by accelerated protons destabilizing the cohesion of the nucleus of the element, which can result in the emission of gamma radiation. This process has an excellent sensitivity and is mostly used for light elements analysis such as Li, B, C, O and F [17]. This restriction of the element is present due to the fact that as the atomic number of the atom rises, so does the magnitude of the repulsive coulomb force of the nucleus, making it more difficult for the proton beam to interact with the nucleus and excite one of the protons or neutrons inside it. While using PIGE exclusively is can be limiting in some cases, it is an excellent complementary analytical technique to other forms of ion beam analysis, such as PIXE (Particle Induced X-ray Emission).

## Chapter 2: Theoretical Background

When dealing with collision of the proton with the nucleus we can subdivide this interaction into three distinct collisions.

- Inelastic Dispersion ( $p, p'\gamma$ )
- Radioactive Capture ( $p, \gamma$ )
- Transfer reaction ( $p, \alpha\gamma$ )

In terms of notation, the left part in the parenthesis represents what is being collided with the nucleus of the atom ( $p$  being a proton,  $\alpha$  an alpha particle and  $\gamma$  gamma radiation), and the right part is what is being attained from this interaction.

The  $\gamma$  radiation is characteristic of the nuclei that emitted it, so with this we can identify and quantify their radiated sample isotopic composition. In this technique, the gamma rays emitted are detected by solid state detectors like the HPGe (High Purity Ge) detectors. The detection limits will vary from element to element tending to round values of 10 and 100 ppm [18]. A typical PIGE spectrum is shown in the following illustration:

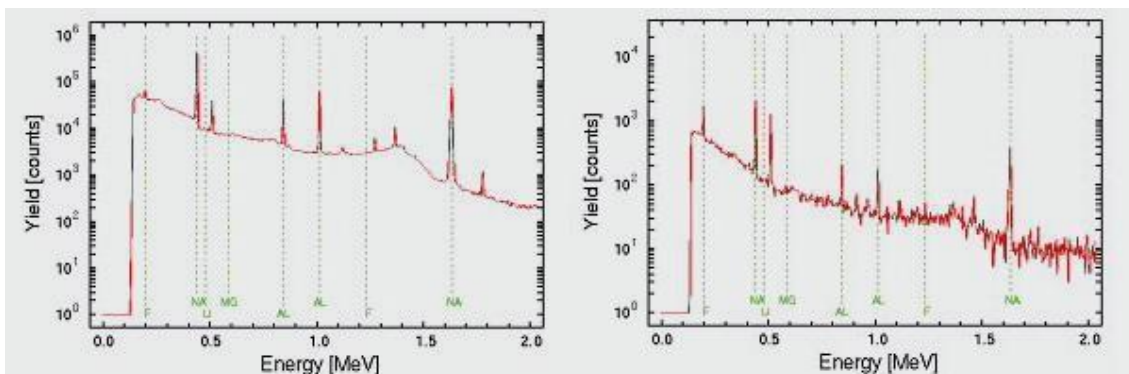


**Figure 2.7** *PIGE spectrum of an archaeological sample (obsidian glass) (left) and PIGE spectrum of an aerosol sample) (right) [27].*

The elements can be identified with their energy and the concentration of each element can be determined by the yield,  $Y$ .

## Chapter 2: Theoretical Background

---

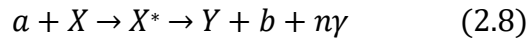
The performance of Gamma emissions,  $dY_i$ , for the gamma ray of the isotope  $i$  present in the sample in the direction of the detector can be given by the equation [25]:

$$dY_i = \frac{Q}{e} f_i N_i(x) \frac{d^2 \sigma_i}{dE d\Omega} dx \Delta\Omega \epsilon_{int} \quad (2.7)$$

Where  $f_i$  is the atomic fraction of the isotope we pretend to detect,  $Q$  the charge of the beam,  $e$  the electron's charge,  $N_i$  the number of particles of the isotope  $i$ ,  $\Delta\Omega \epsilon_{int}$  is the efficiency of the detector for a given photon, and  $\sigma_i$  is the cross section of the given element.

### 2.5.2 Nuclear Reaction Analysis

Nuclear Reaction Analysis (NRA) is a nuclear method for the quantitative determination and depth profiling of selected light elements and isotopes. This method shares a lot of similarities with Rutherford Backscattering fleshed out in chapter 2.2.3. In the interaction with a nucleus, a nuclear reaction occurs producing charged particles, neutral particles, or photons. A nuclear reaction can be expressed as [25]:



Where  $a$ , would be the incident particle nucleus of mass colliding with nucleus  $X$ . After this collision we have the formation of an unstable compound  $X^*$ , this instability results in the formation of a new nucleus  $Y$  and the emission of a particle  $b$  and  $n$  photons  $\gamma$ .

The excess of kinetic energy (Called the Q-Value) can be given by the equation, where  $E_g$  represents any given energy of a  $g$  particle in the equation 2.8, for example,  $E_Y$  represents the energy of the new nucleus  $Y$  in equation 2.8,  $E_b$  represents the energy of the particle  $b$ ,  $E_\gamma$  represents the energy emitted by the reaction process,  $E_a$  the energy of the colliding particle and  $E_x$  the energy associated with the original nucleus. [25]

$$Q = E_Y + E_b + E_\gamma - E_a - E_x \quad (2.9)$$

## Chapter 2: Theoretical Background

An example of this can be seen below using an ion of  ${}^3\text{He}$  colliding with  ${}^2\text{H}$ .

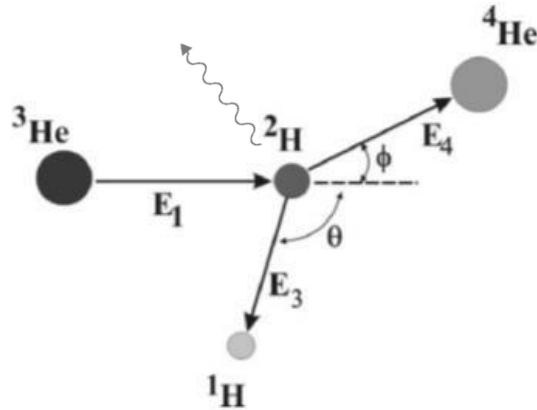


Figure 2.8 - Collision of a  ${}^3\text{He}$  with a  ${}^2\text{H}$  resulting in a  ${}^4\text{He}$ , a  ${}^1\text{H}$  and a photon. [25]

Now, depending on the Q-Value of the reaction we can have either an endothermic (if  $Q < 0$ ) or exothermic ( $Q > 0$ ) reaction.

An example of a nuclear reaction can be seen in Fig. 2.10, which depicts the fusion reaction cross section of protons with  ${}^{18}\text{O}$ , producing  ${}^{15}\text{N}$  and an alpha particle [1]

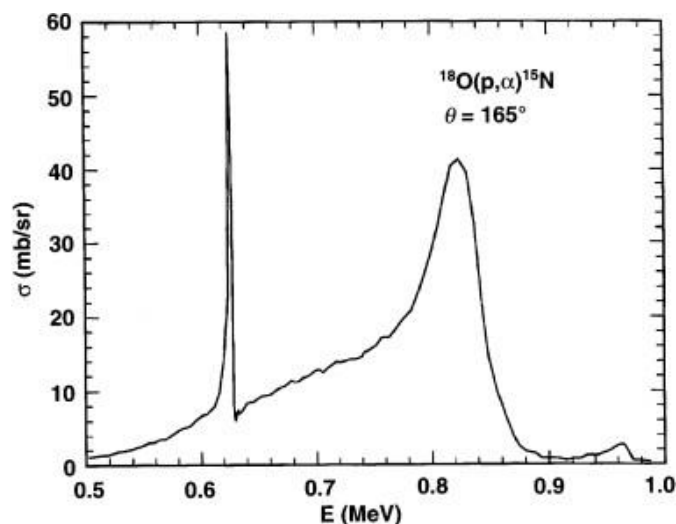


Figure 2.9 - Cross Section for the  ${}^{18}\text{O}(p, \alpha){}^{15}\text{N}$  reaction at  $165^\circ$  [1].

This spectrum gives us the cross section of the element throughout different energies

# Chapter 2: Theoretical Background

## 2.5.3 Rutherford Backscattering Spectroscopy

RBS or Rutherford Backscattering Spectrometry relies on Rutherford Scattering, already discussed in subchapter 2.1.1.

This technique requires the usage of a particle accelerator and can be utilized to determine not only the distribution of superficial elements (typically in the range of dozens of  $\mu\text{m}$ ), but it can also determine the structure of the sample being analyzed.

The sample is bombarded by charged particles (typically  $^4\text{He}^+$ ) that are dispersed elastically by the nucleus of the analyzed sample, and the backscattered beam of high energy ions is analyzed. The lost energy depends on the atomic number ( $Z$ ) of each element of the sample [19].

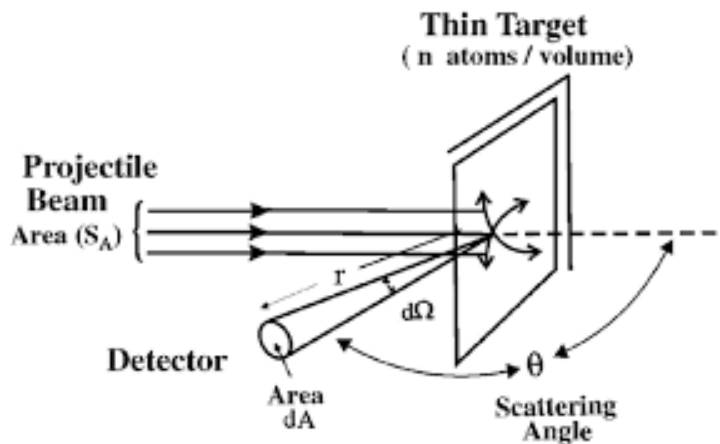


Figure 2.10 - Example of an RBS experiment [19].

The RBS technique is widely used for near-surface layer analysis of solids and is useful to determine the profile of concentration vs. depth for heavy elements in a light material as a function of the detected energy. RBS using deuteron beam has been found to be a useful compromise between proton and  $\alpha$ -particle RBS for the thicker layers often encountered in art and archaeology [20].

# Chapter 2: Theoretical Background

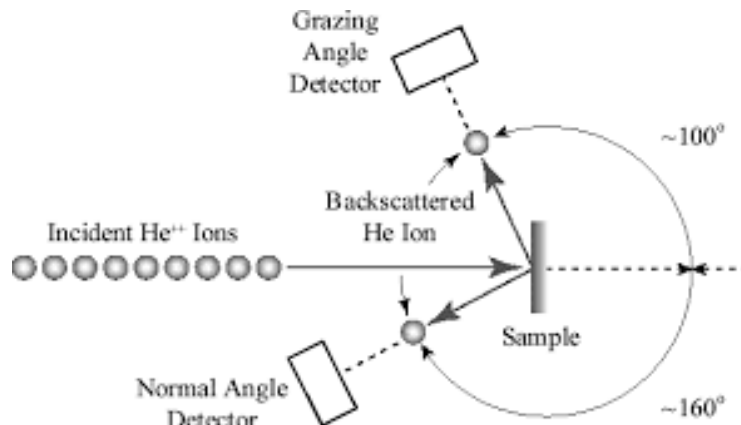


Figure 2.11 - Schematic of RBS experiment. [28].

## 2.5 - Faraday Cage

A Faraday Cage can be described as an enclosure that is utilized to block electromagnetic fields. Any external electrical field causes the electric charges within the cage's conducting material to be reorganized in such a way that the field inside of the cage is nullified, this can be used to protect the equipment, but in this work the construction of the cage had the goal to nullify external noise [21].

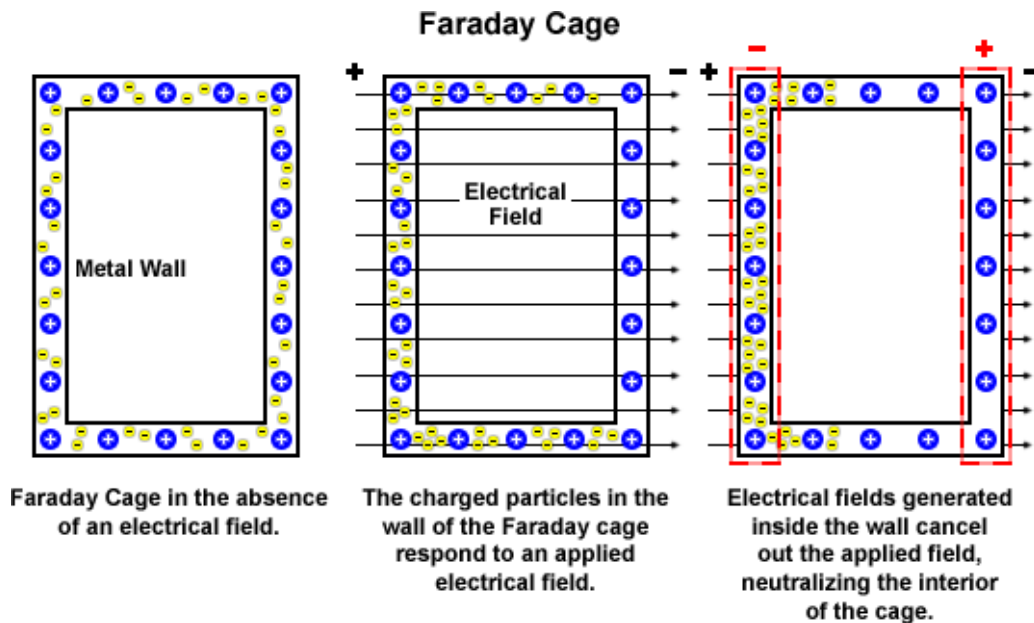


Figure 2.12 - Visual representation of the reorganization of the charges of the cage's walls in response to an exterior field [21].



## Equipment, Materials and Methods

This chapter is divided in two parts, the first part refers to the equipment that is present in CTN, and secondly a discussion of the material that was constructed/purchased for the construction of the system, including the new Faraday Cage constructed for this project.

Moreover, each designed part has their related 2D technical drawing available as an annex to this document, STL models can be provided if requested to the author.

# Chapter 3: Equipment, Materials and Methods

---

## 3.1 Present parts

As stated earlier, this subchapter discusses the present parts and machinery present in CTN, this is important not only for dimensioning the new parts that will be acquired, but also to give a deeper understanding of the physics behind the equipment.

### 3.1.1 Tandem accelerator



**Figure 3.1: CTN tandem accelerator.**

What differs a tandem accelerator from a typical electrostatic accelerator is the fact that these have a two-step acceleration of ion particles utilizing a single high voltage terminal. Much like the typical electrostatic accelerator, the tandem accelerator starts with a low voltage (in the range of hundreds of volts) at the start of the line and ramps up to a very large voltage (in the range of the Megavolts). The case of the CTN tandem, we have an accelerator with voltage values in between 500kV and 3 MV depending on the type of experiment being conducted [22].

# Chapter 3: Equipment, Materials and Methods

---

## 3.1.1.1 Duoplasmatron ion source

The main idea of the ion source is the possibility of creating ions that will be accelerated by the rest of the system. The ions source utilized for the experiments is that of a Duoplasmatron ion source. The Duoplasmatron ion source is a modified Von Ardenne in which a cathode filament emits electrons into a funnel shaped electrode that is constricted by an anode and a cathode. Gas to be ionized is injected into this chamber as displayed in Fig. 3. 3.. A strong magnetic field is developed between the anode and cathode, which constrains the discharge to a narrow plasma beam along the axis of the exit aperture. The nature of the of the ions can be changed by switching the gas source entering the electrode. For example, as described by Hugo Silva [24] to produce a proton beam, we can utilize a hydrogen container. For oxygen, a CO<sub>2</sub> container.

The ion source can produce H<sup>-</sup> and oxygen beams, these beams have intensities up to 30 μA. The Duoplasmatron ion source is managed by several power supplies and meters:

# Chapter 3: Equipment, Materials and Methods

Filament (up to 20 A), Magnet Control ( $\approx 0.5A$ ), Gas Control (a.u.), Extraction Voltage ( $\approx 100V$ ), Extraction (1 mA) and High Voltage Power Supply (15 kV) [25].

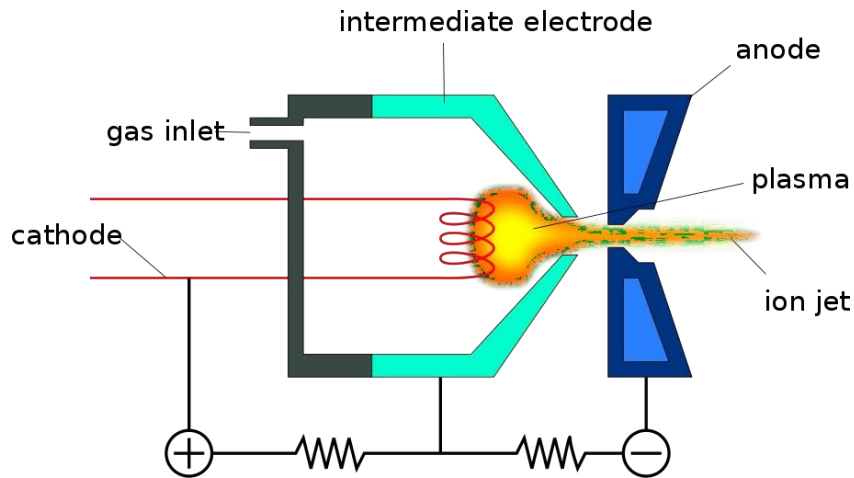


Figure 3.2 - Labeled Schematic of an Duoplasmatron ion source [27].

## 3.1.1.2 Beam transport system

The transport system is divided into two different stages based on the energy of the particles, the first of which is present before the acceleration tank (from now on referred to as Low Energy (LE)) and a second stage after the particles have passed the acceleration channel, the system is represented in Fig 3.3.

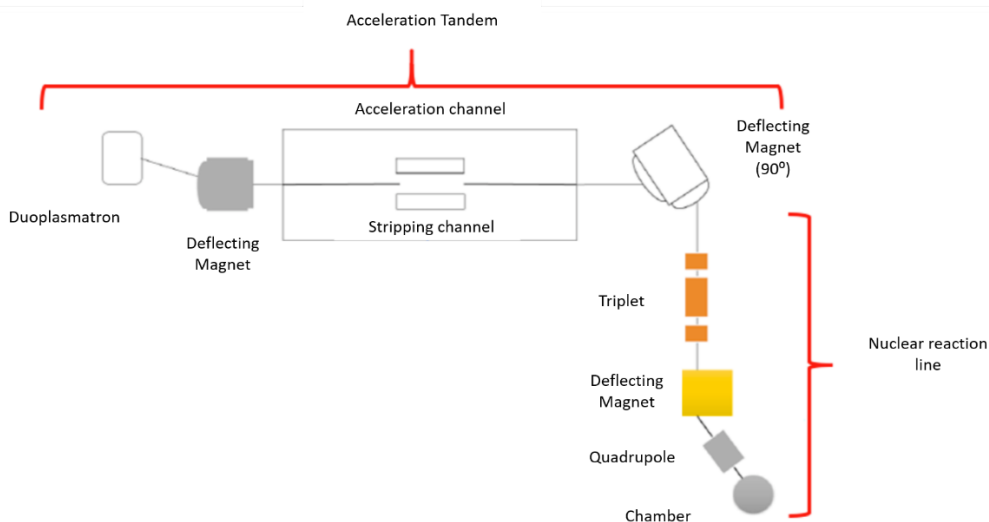
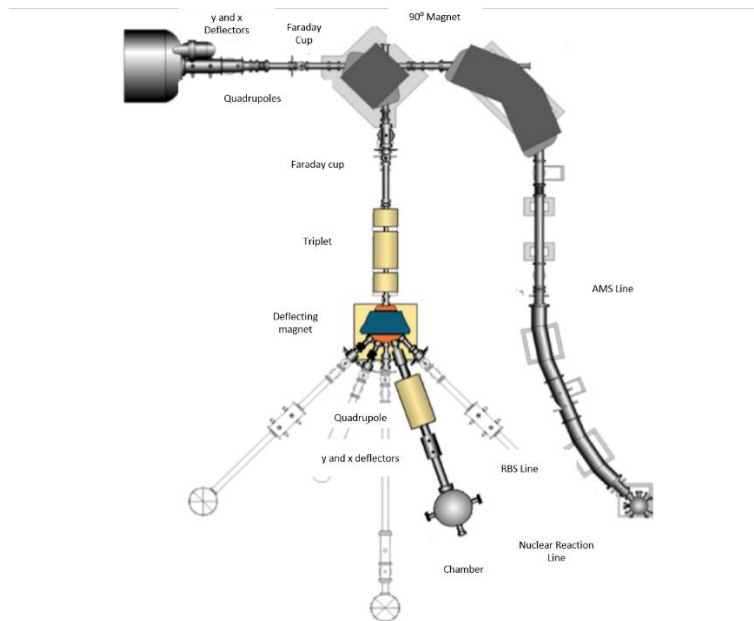


Figure 3.3 –Diagram of the nuclear reaction line of the tandem accelerator, adapted from [3].

## Chapter 3: Equipment, Materials and Methods

The LE segment is constituted by the duoplamatron source, described in the previous subchapter and the low energy switch, this switching magnet makes the mass to charge ratio ( $m/q$ ) filtration of the ions that will enter the accelerator.



**Figure 3.4 –Diagram of the nuclear reaction line after passing the tandem accelerator, adapted from [3].**

After being accelerated by the Tandem, the beam is focused by the Electrostatic Quadrupole located at the exit point of the accelerator (Fig 3.4). The beam has its current measured by the Faraday Cups before and after being deflected by the 90° Magnet.

Triplets are positioned after the measurement of the beam to properly focus it, following that the beam is redirected to the Nuclear Reactions line by the deflecting magnet where it be utilized for the experiments.



**Figure 3.5 –Tandem's nuclear reaction line**

# Chapter 3: Equipment, Materials and Methods

## 3.1.1.3 Beam transport chamber

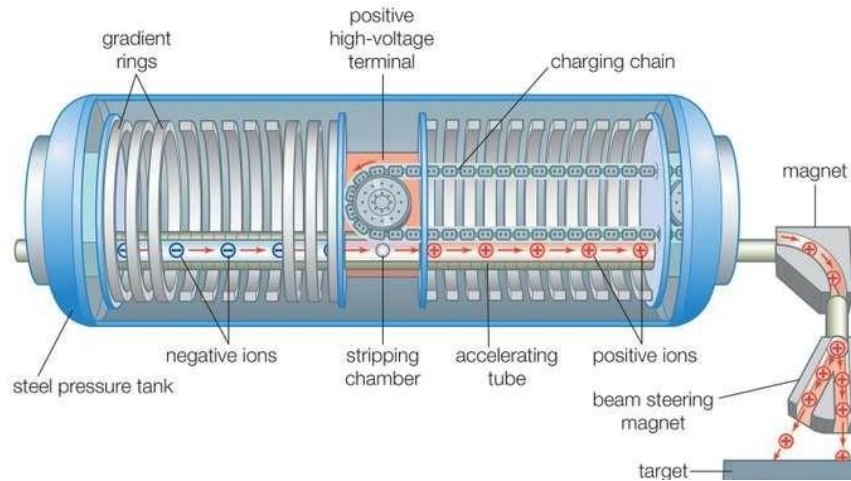


Figure 3.6 - Labeled internal image of a tandem accelerator [23].

After exiting the previous chamber, the particles of interest will have to be injected into the accelerator, stripped, and accelerated into the vacuum chamber where the experiment will be conducted.

## 3.1.1.4 Stripping

In this context, stripping is the process of removing the electrons of the outer layers of the ions constituting the incoming beam. This is important, the removal of electrons makes the particle positive, this way we can accelerate the same particle two times with the same voltage source, as we can see in the fig 3.8 the negative ions are initially accelerated by being attracted to the Positive High-voltage terminal, after being stripped and becoming positive ions they are now repulsed by the positive high-voltage terminal. This results in an energy that exceeds the initial by both the type of stripped ion formed, and voltage applied by the Positive High-voltage terminal, this can be quantified by  $E_f = E_i(q + 1)e \times V_t$ , where  $E_f$  is the energy that the particle will have at the exit point of the tandem,  $E_i$  is the energy that particle initially has,  $q$  is the charge the particle has at the end of the stripping process and  $V_t$  is the voltage applied to the terminal. So for example,  $^{110}\text{Ag}^{7+}$  ions will achieve a final energy of 24 MeV at  $TV = 3 \text{ MV}$ .

# Chapter 3: Equipment, Materials and Methods

The removal of the electrons is achieved by colliding the beam of ions through a gas, the present stripping chamber keeps around 1 to 2  $\mu\text{g}/\text{cm}^2$  of gas in its chamber as the beam passes through. The state of the ions exiting the stripper channel depend on multiple factors that will affect the stripper's efficiency, factors such as the gas itself, it's pressure and the terminal voltage of the accelerator [22].

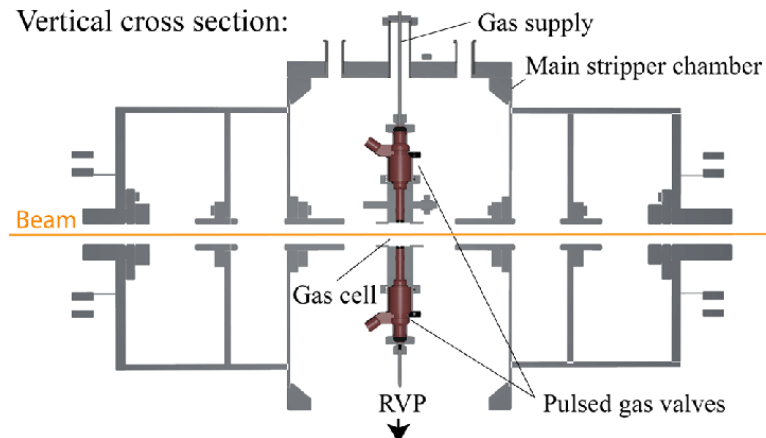


Figure 3.7 - Cross section of a stripping chamber [22].

### 3.1.1.5 Nuclear Reaction Chamber

At the end of the line there is a vacuum chamber, the installation of the faraday cage and the sample holder will take place in this part of the nuclear reaction line. To properly install the new Faraday Cage, further discussed in chapter 3.2.1, some design limitations are presented by the chamber's own parts represented in Fig 3.7. These include:

- **The detectors**

Within the nuclear chamber, a total of 3 detectors were considered when designing the faraday cage: A gamma detector, and two particle detectors.

The gamma detector is a hyper pure Germanium crystal (HPGe) with 65 mm in diameter and 62.6 mm in length covered in a 1mm thick aluminum cover present at 55.5 mm from the target sample and in an inclination of  $130^\circ$  from the beam. The detector is cooled with liquid Nitrogen [2].

The particle detectors, referred to from now on as PIPS (Passivated Implanted Planar Silicon) can move in an angular fashion and have their movement controlled from the outside of the chamber.

## Chapter 3: Equipment, Materials and Methods

---

- **Collimator system**

Located at the entry point of the chamber, this system allows the measurement of both the current and width of the beam. This part is represented in Fig 3.6.

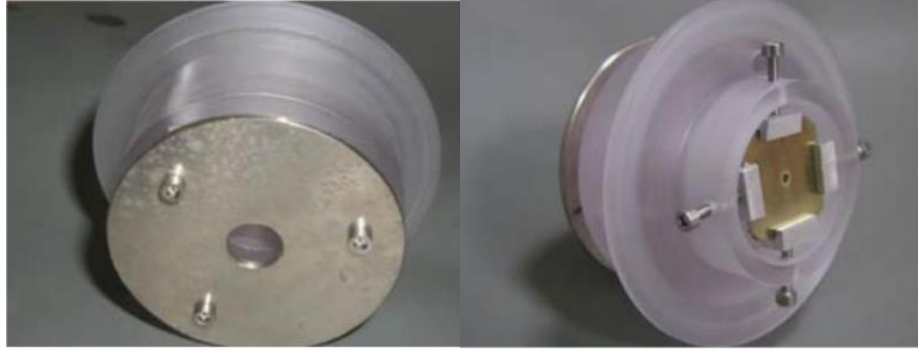


**Fig 3.8 – Photo of the nickel plate that protects the nuclear reaction chamber without the inclusion of the golden plate(left) and photo of the nickel plate that protects the nuclear reaction chamber with the inclusion of the golden plate(right). Taken from [1]**

- **Beam stopper**

Constructed out of stainless steel AISI304, this part has the objective of preventing the backscattering of particles back into the detectors.

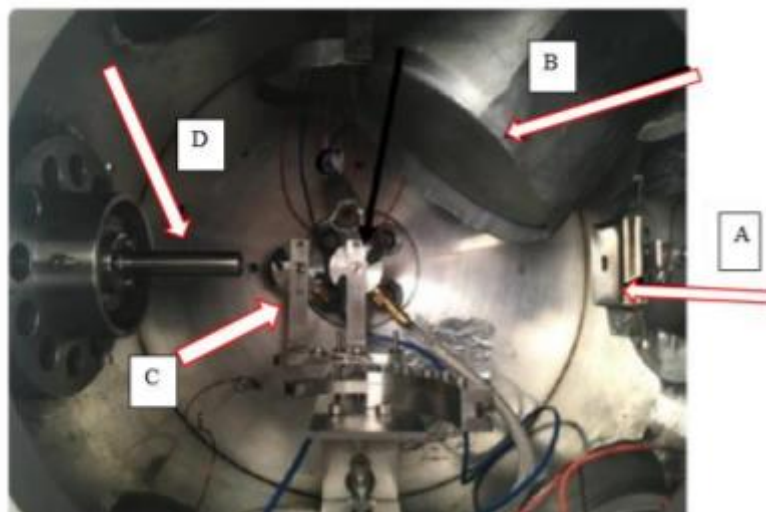


**Fig. 3.9 - Photo of the interior of the nuclear reaction chamber with the referred parts. A-Collimator system; B-Gamma detector; C- PIPS detector; D-Beam stopper, the beam enters the chamber through A and has the direction of D adapted from [1].**



# Chapter 3: Equipment, Materials and Methods

---

## 3.2 Acquired parts

This subchapter is dedicated to the parts that were either constructed or purchased for this project.

### 3.2.1 Faraday Cage

In 2.6 we discussed some of the basic notions of the Faraday Cage, with this in mind we can now discuss the construction of the new faraday cage.

When designing the new cage, a certain number of parameters had to be taken into account:

- The size of this new cage must be able to fit inside the vacuum chamber with all the machinery inside of it (detectors, beam stopper etc.)
- As in chapter 2, must be constructed of a conductive material
- The lid must have a hole to fit the new sample holder, not too big that it takes away the cage's properties
- The proton beam must go through the centre of the cage that coincides with the centre of the vacuum chamber
- The electron cannon must be positioned in such a way that the electrons will collide with the sample to discharge it.
- Cables associated with the detectors must be able to enter the cage
- The feet of the cage must be sized to hoist up the cage in a way that coincides with the centre of the incident proton beam.

Taking all these points into account, the design bellow was conceived, to achieve a better understanding of it, a labeled transparent version of it is presented as well as a non-transparent version.

## Chapter 3: Equipment, Materials and Methods

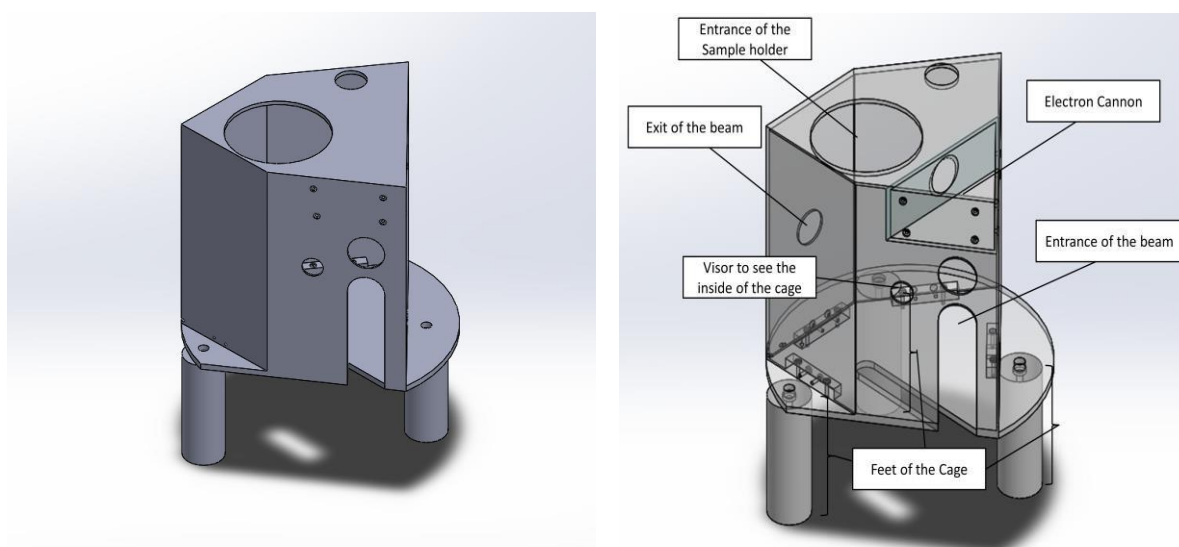


**Figure 3.10 - Labeled representation of the new Faraday Cage (right) and non-labeled version of the cage (left).**

In the front of the cage, an inverted U-shaped hole is presented, the beam enters the top of the structure, and exits the circular hole at the back of the faraday cage. At the exit point of the beam, the beam stopper is located, the beam stopper is a cylindrical-shaped part with the goal of retaining the beam, with multiple reflections of said beam inside the structure slowly decreasing its energy halting it after a period of time. This is important to prevent the further interaction of the beam with the rest of the samples. This guarantees that the proton beam doesn't interact with the rest of the samples, nor with the same sample multiple times. The hoisting of the faraday cage was made possible through the usage of M5 threaded rods, the rods were screwed at the bottom of the vacuum chamber and at the holes presented in Fig. 3.1, these rods will be referred to as the "feet" of the cage.

In order to assure a complete electrical isolation of the faraday cage, its necessary to isolate it from the rest of the vacuum chamber, since it's made out of conductive material it would interfere with the results obtained. With this said, the electrical isolation between the feet and the cage is necessary, the solution was to introduce small Macor rings in the contact between the cage and the feet, assuring the complete isolation of the cage throughout the experiment.

## Chapter 3: Equipment, Materials and Methods

---

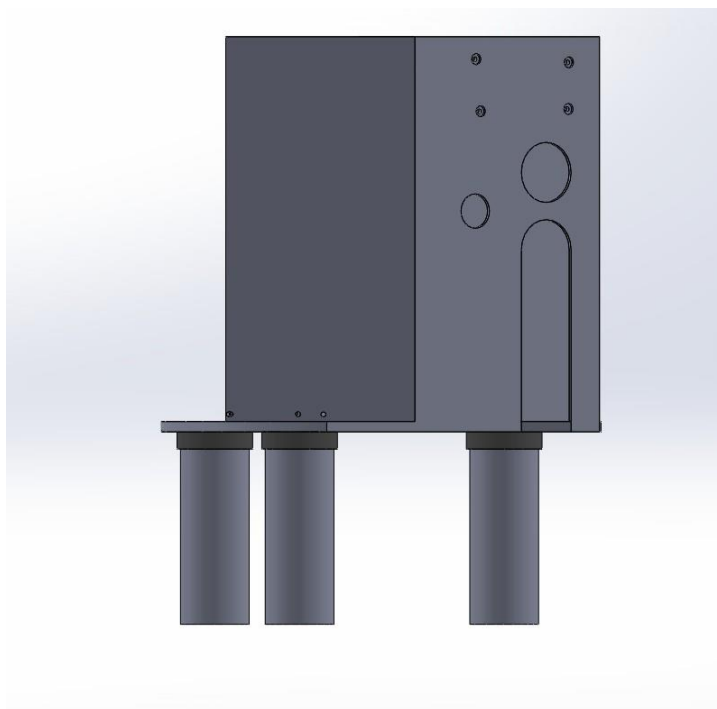


**Figure 3.11- Electrical isolation of the Faraday Cage.**

The bottom of the old Faraday Cage was reutilized, with some small modifications, namely the increase in size of the gap present for the introduction of detectors. This proved to be useful since it matched the size of the new cage and the holes that were present in this aluminum piece matched the holes at the bottom of the vacuum chamber for the rods to be screwed onto.

When a particle beam collides with an isolating sample, even when dealing with a small current of a few nA, the risk of sparks arises, these electrical sparks go from where the beam is colliding with the sample and the nearest conductive surface. This can cause the production of secondary electrons and damage the results. In order to avoid these incidents, the incorporation of an electron cannon was taken into account when designing the Faraday Cage.

This electron cannon consists of a conductive filament made out of tungsten, the emission of electrons is possible through thermo-electrical effect when a current goes through it and an extraction grid that has to be polarized and positioned between the filament and the target allowing the acceleration of the electrons towards the sample being analyzed. The Faraday cage has enough room for the electron cannon to be bolted to it and be properly aimed at the sample.

## Chapter 3: Equipment, Materials and Methods

---

The construction of the Cage was done in the FCT workshops, they were also responsible for the alterations to the base of the old faraday cage. The cage consists of two different plates, two different lids with different hole sizes for different sample holders, a smaller one with a 40-millimeter opening for the old sample holder, and a larger one with 55 millimeter opening for the new sample holder, all of them made out of copper with a thickness of 1 millimeter. All the technical drawings for both walls and the lids are included as an annex to this document.

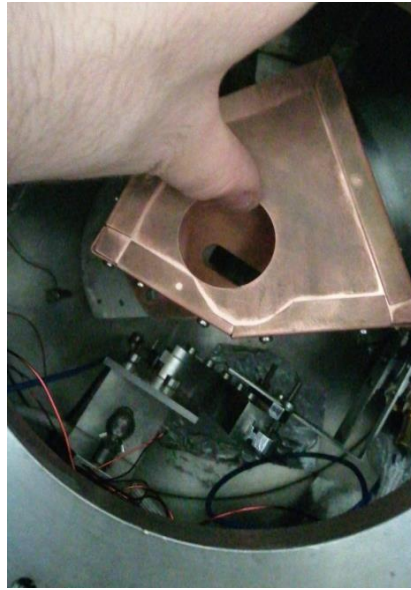


**Figure 3.12 - Installed Faraday Cage.**

The faraday cage must be positioned vertically very precisely, and the movement of a few millimeters can compromise the position of the proton beam when colliding with the sample. In order to properly fixate the faraday cage, nuts were welded into the different rods that supported the faraday cage at approximately four millimeters of the bottom of the vacuum chamber, due to the tight space on the chamber, these bolts are not visible in the image above.

# Chapter 3: Equipment, Materials and Methods

---

## 3.2.2 Sample Holder

The new sample holder aims to correct some of the flaws that existed with the old one, namely the lack slots to insert a large amount of samples. When designing this new sample, certain aspects were taken into account.

- The current laminal sample holders already present in CTN must fit the sample holder
- The shape of the sample holder must have an uneven number of points so that we can have the beam go through the sample holder without having the beam interacting with other samples
- Must have a sufficiently large amount of sample slots to justify its construction

Initially the proposed design was that of a pentagon, however with sizing limitations, the necessity to cut back was necessary, with this said the sample holder designed was that of a triangle. Below a labeled image of the sample holder can be seen.

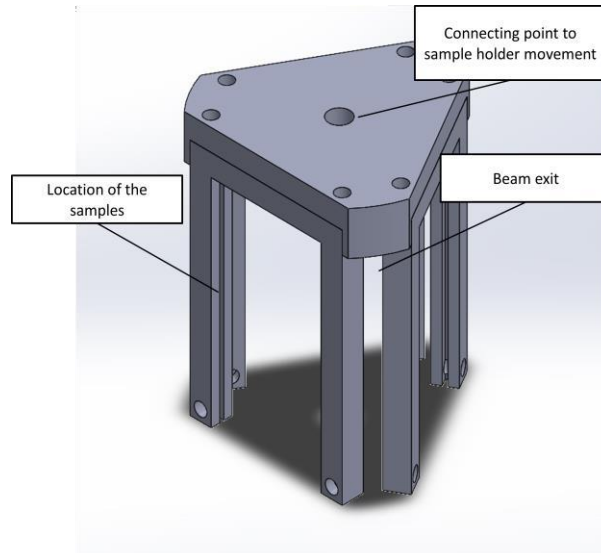


**Figure 3.13 - Labeled representation of the sample holder.**

Samples are loaded into small lamels like the ones presented in Figure 3.12 and then slotted into the C shaped areas of the sample holder. The 3 C shaped edges of the sample holder can be detached from the larger part, making it easier for samples to be inserted into them, and later on bolted with M3 bolts into the sample holder.

## Chapter 3: Equipment, Materials and Methods

---



**Figure 3.14 - Removable C shaped edge.**

The sample would be placed into the circular hole (fig) and fixated with the bolt and the bottom of the sample holder and aligned with the beam, the center of the vacuum chamber and the beam stopper. The beam would collide with the sample and exit through the back of it ending up inside of the beam stopper, not interacting with any of the other samples of the sample holder. The electrical isolation of the sample holder is also necessary, this can be achieved with the usage of a isolating material in the "connecting point to sample holder" area of Fig 3.8.

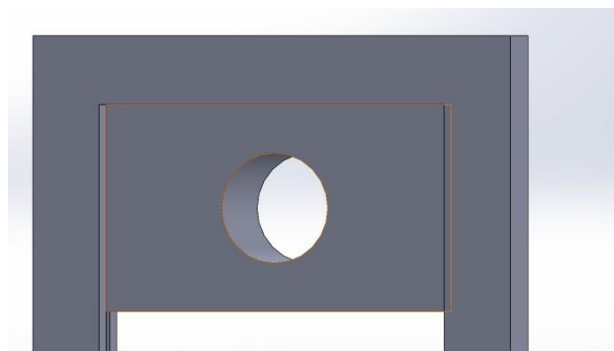


**Figure - 3.15 Example of a laminal sample holder inserted.**

Nearing the center of the sample holder, a small bolt was inserted so that the charge of the samples can be collected, the code was adapted for this, something that isn't desired is for the string to interlace with the vein

## Chapter 3: Equipment, Materials and Methods

---

connecting the sample holder to the motorized movement enablers. In order to achieve this the coding was developed in such a way that the sample holder wouldn't rotate over 360° this minimizes the risk of contact of the string with the vein outside of the isolating area.

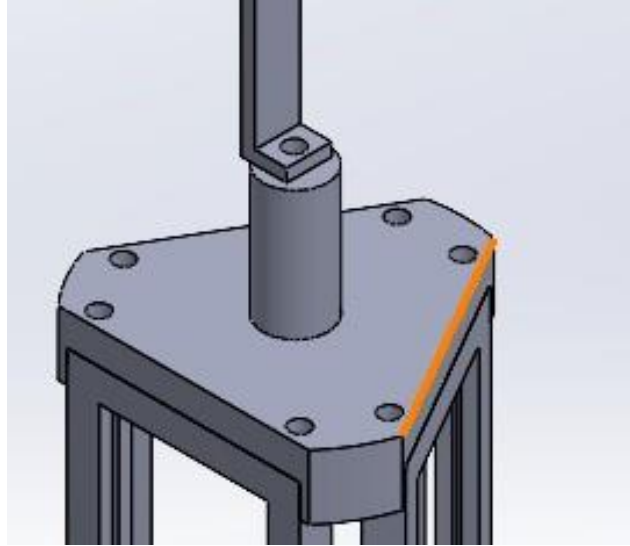


**Figure 3.16 - Connection vein attached to isolation area.**

# Chapter 3: Equipment, Materials and Methods

---

## 3.2.2.1 - Sample holder past designs

For this project a total of 5 sample holder designs were submitted, this chapter discusses the reasons why some of them weren't chosen for the final project, and presents them as a way to provide a record of their existence.

This was the first design submitted, the main idea was to have fixed locations for the samples, this however presented some problems

- For one although it presented a fixed position to place samples it was incompatible with the old lamele where the samples are placed
- The vertical squares proved to be too frail to be manufactured
- Too complex to be manufactured

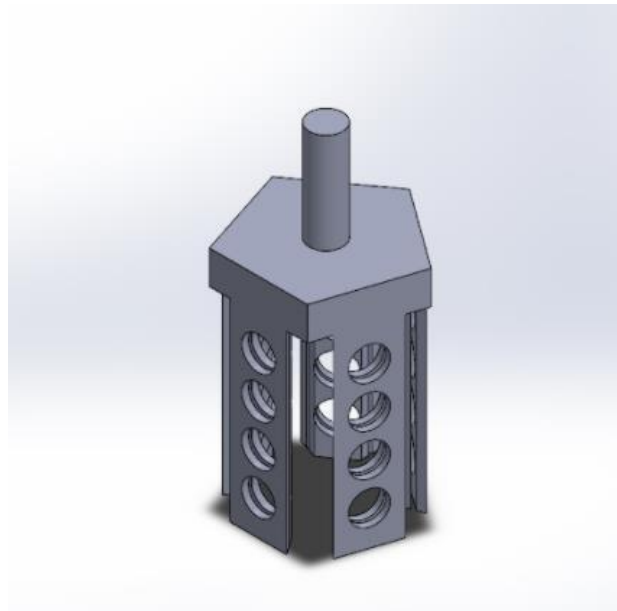


**Figure - 3.17 First design.**



## Chapter 3: Equipment, Materials and Methods

---

The second design also proved to be too complicated to be manufactured, the legs were also too frail to be consistently constructed, following this the new proposed design was proposed with thicker legs.

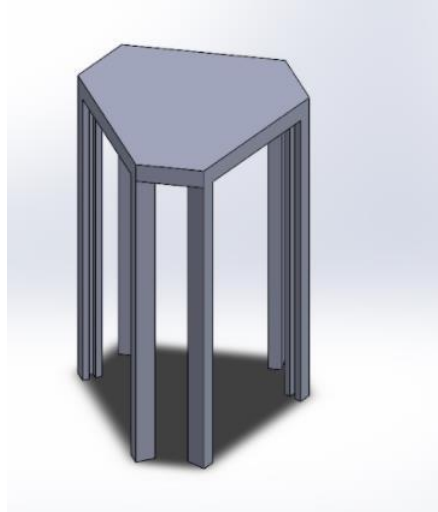


**Figure - 3.18 Second design.**

This was a more finalized design, the problem of this sample holder was how large the radius of the sample holder would be as it couldn't fit through the lid of the faraday cage, another problem was with the legs, the construction could prove difficult if the whole part were to be constructed as a single part.

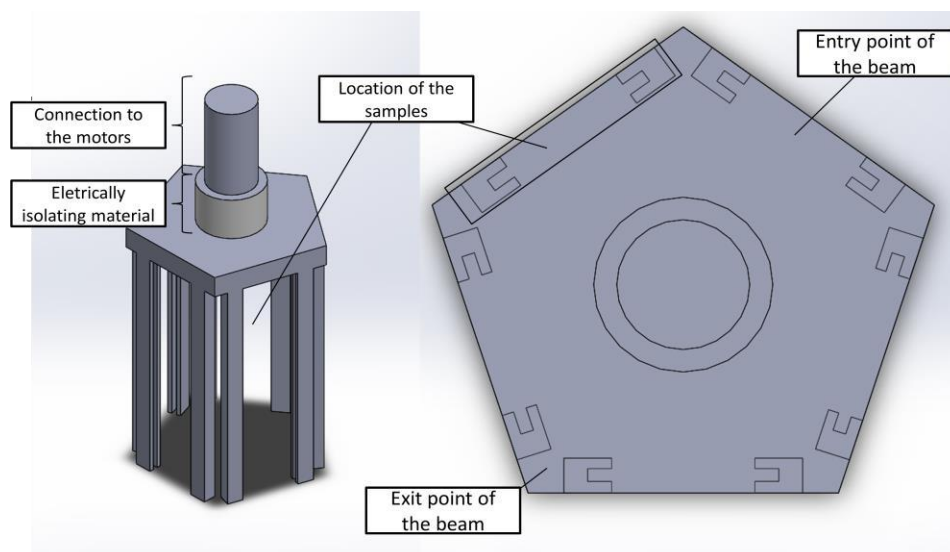


**Figure - 3.19 Third Design.**

## Chapter 3: Equipment, Materials and Methods

---

This design was the one proposed by the workshop that the parts were constructed, the design had the flaw that the old lamellas could not be placed inside of this design, so it was discarded.

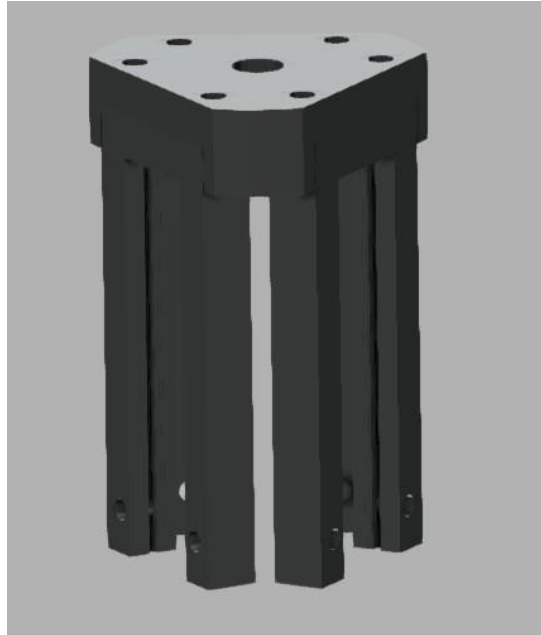


**Figure - 3.20 Design presented by the workshops.**

The final design utilized bits and pieces from all of the above designs and is the one presented in 3.2.2.

### **3.2.3 Sample holder motion**

The sample holder is designed to have 2 degrees of freedom, angular discussed on chapter 3.2.3.1 and a linear one discussed in 3.2.3.2, both these parts were purchased to the manufacturer LewVac. The system is located on the outside of the vacuum chamber, and the automatic motion of these parts is allowed with motors controlled with an Arduino board, the code is discussed in chapter 4.

# Chapter 3: Equipment, Materials and Methods

## 3.2.3.1 Angular Motion

Angular motion is achieved utilizing a Two Stage Differentially Pumped Rotary Platform provided by LewVac [24], this part is capable of rotating the sample holder either manually or with the usage of motors.

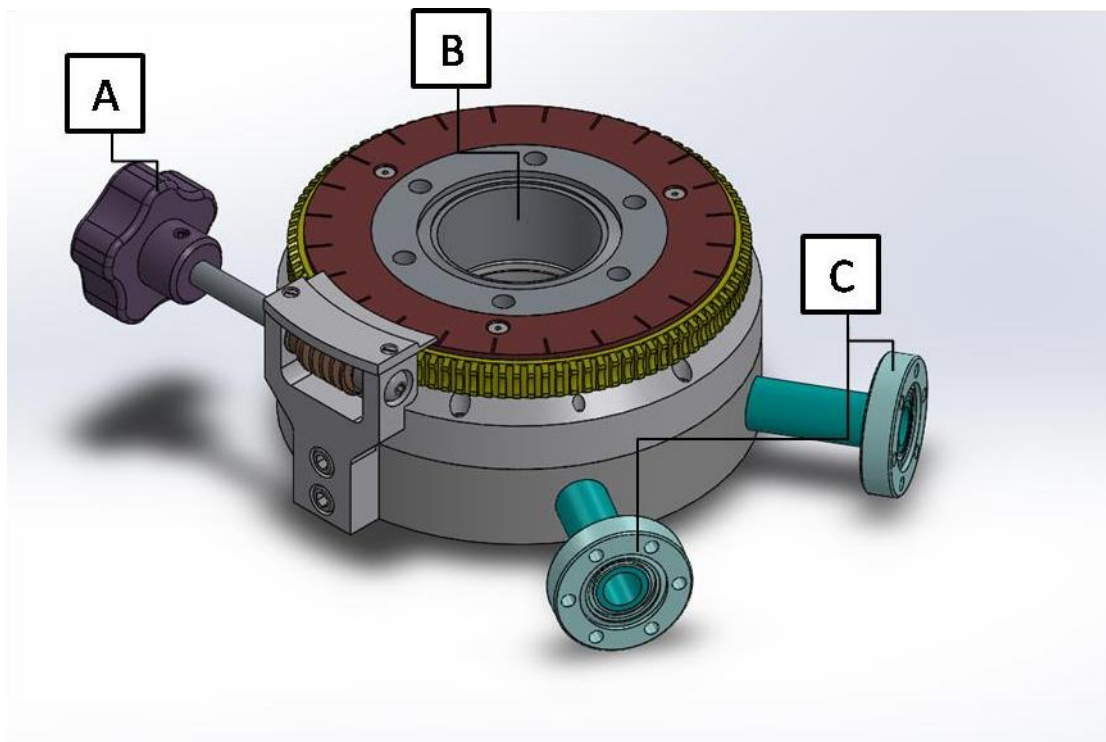


**Figure 3.21 - Labeled Rotary platform.**

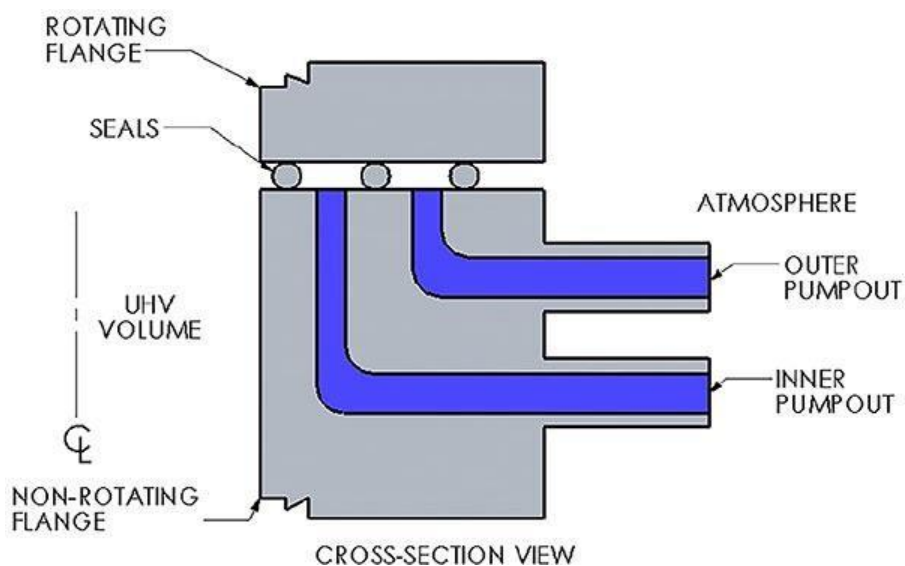
The rotation is achieved by rotating the handle [A], this handle can be removed and allow the insertion of a motor to automatically rotate the sample holder. The part allows the placement of vacuum tubes in [C] since the part has to be maintained at a vacuum, this part has six holes on each side that are connected on one end to the linear feed through and on the other to the lid of the vacuum chamber. The linear feed through, discussed in the next subchapter, passes through [C] and connects to the sample holder.

Fig 3.18 represents the cross section of the Two Stage Differentially Pumped Rotary Platform (TSDPRP).

The fluorocarbon seals can withstand a differential pressure of about  $1.33 \times 10^{-7}$  mbars. Differential pumping can increase the range of a single seal significantly to maintain true ultra-high vacuum pressures. For instant, providing rough pumping ( $\sim 1.33^{-3}$  mbar) in the Outer pumpout volume and moderate pumping on the Inner pumpout volume, results in a pressure differential between UHV and the Inner volume of  $1.33^{-5}$  torr but virtually no

## Chapter 3: Equipment, Materials and Methods

pressure differential to drive gas molecules across the seal. The result is a leak-tight, yet rotating, seal.



**Figure 3.22 - Cross section of the Rotary Platform [25].**

The device rotates continuously in either direction, as it rotates the pressure increases slightly in the proximity of the DPRP, this occurs to the friction between stainless steel and the seal. Mass spectrometer studies show the bursts to be mostly water, methane, CO, and CO<sub>2</sub> with small amounts of H<sub>2</sub> [25].

# Chapter 3: Equipment, Materials and Methods

---

## 3.2.3.2 Linear Motion

The linear motion of the sample holder will be achieved with the linear feedthrough ordered from LewVac [25]. The size of the bellow was chosen so that it would be capable of moving through the totality of the Faraday Cage. Much like the rotary platform, this part can both used manually or with the usage of motors, the motors are connected to the top of the linear feedthrough.

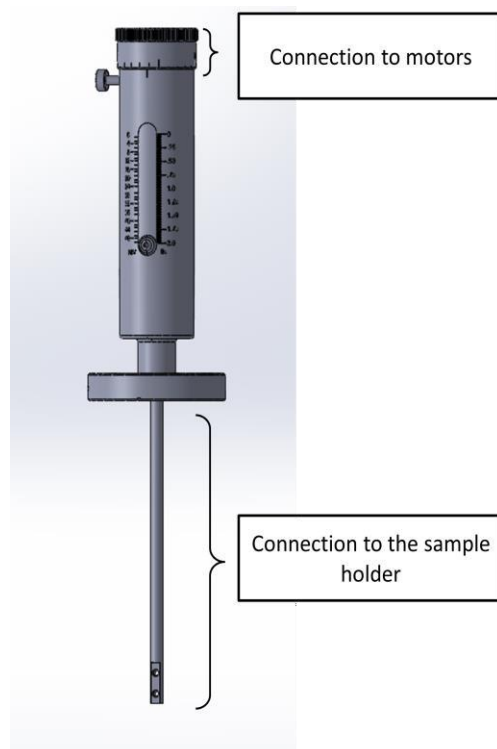


**Figure 3.23 - Labeled Feedthrough.**

# Chapter 3: Equipment, Materials and Methods

---

Like stated in 3.2.2 the connection from the linear feedthrough to the sample holder is achieved with a rod of 45 mm, at the top of the rod, the linear feed through is connected via the 2 holes represented in Figure 3.21.

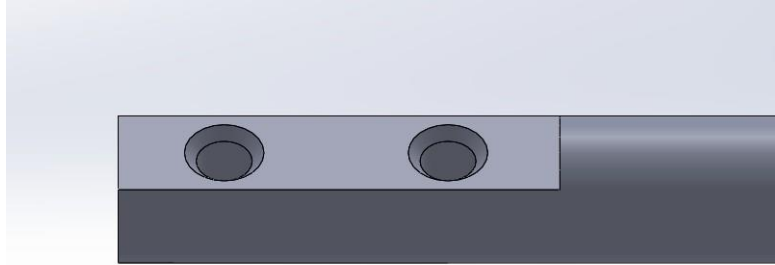


**Figure - 3.24 - Connection to the rod stated in chapter 3.2.2.**

Both the linear feedthrough and the rotary platform have a CF40, so the connection of both is a fairly simple process, both the parts were made by the same manufacturer, and thus have very low risk of not being capable of properly attaching to one another.

Bellow a SolidWorks representation of both parts is displayed,

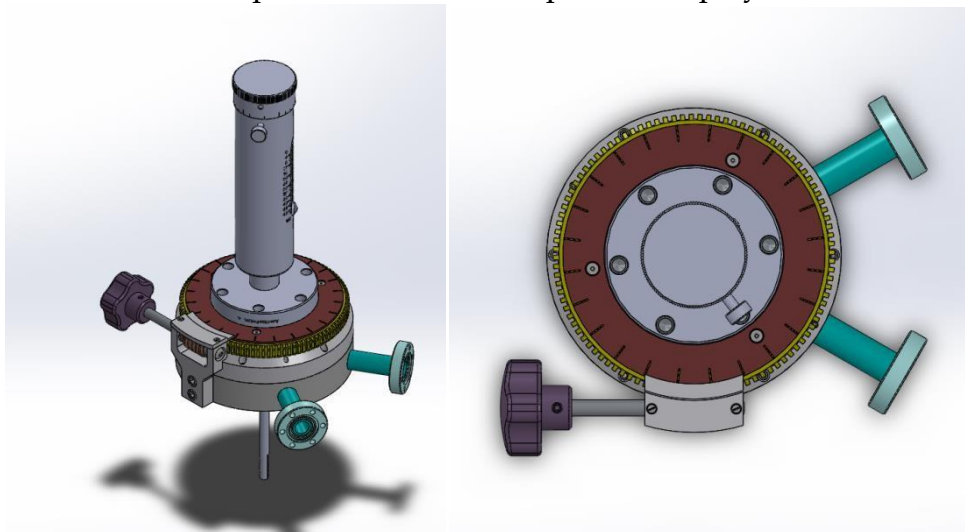


**Figure - 3.23 - Representation of both parts properly attached to one another, from the side represented on the left, and from the top represented on the right.**

# Chapter 3: Equipment, Materials and Methods

---

## 3.2.4 New Lid

For this project the redesign of the lid of the vacuum chamber was also necessary. This new lid must have a new hole a few millimeters from the centre in order for the sample holder to go through, this is necessary since the position of the samples needs to be centered for the detectors to maximize the efficiency of the results. At the top of the new lid an o-ring matching the one on LewVac's rotary platform is necessary, and at the bottom of the lid the old rubber o-ring can be utilized, the bolts on the lid were placed in a way to coincide with the holes in the vacuum chamber this way it can be bolted to the chamber much like the old one. At the laterals of the lid, handles were welded to assure an easier way to transport the part. Bellow an image of the lid is presented, from a top-down perspective (left), and a bottom-up perspective.

The tube visible on the image to the left exists for two reasons, firstly to be capable of welding the CF40 properly to the bottom disk, and secondly this distance allows for a proper movement of the sample holder through the vacuum chamber to swap between samples.

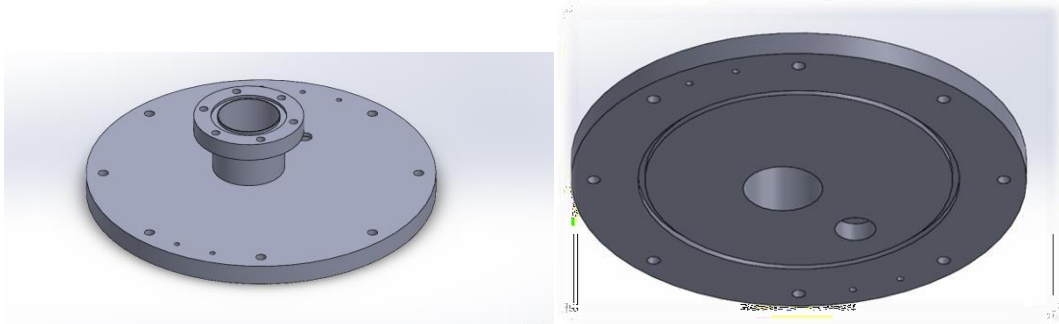


**Figure - 3.25 3D Modelling of the new Lid.**

## Chapter 3: Equipment, Materials and Methods

---

In Fig 3.22 the hole A exists so that the insertion of a BNC, the BNC represented in fig is connected to the sample holder and collects the charge to be analyze



**Figure 3.26 - Typical BNC connector [29].**



CHAPTER



# 4

## Code structure

This chapter is dedicated to the code of the motors, it discusses both the interface that is provided to the end user (that will be referred to as GUI) and the inner workings of the code.

The code is in Python and C++. Python was utilized to code the GUI and C++ to program the Arduino that will be connected to the motors.

This chapter also provides a step-by-step guide of navigating the program.

All the imagery of the GUI was done in Microsoft's Paint.

Much like the technical drawings, the code will be provided as an appendix to this document.

# Chapter 4: Code Structure

---

## 4.1 Graphical User Interface

The GUI has two modes, a Standard mode and Manual mode. The standard mode is designed for the fixed positions of the sample holder that was made during this work.

The Manual mode can incorporate any sample holder, and thus the required positions of the samples need to be provided for the motor to move properly.

When initializing the program, the user is presented with the following menu:



**Figure 4.1 - Initial menu to choose between two modes.**

The following subchapters will explain each mode in more detail.

## 4.2 Standard Mode

As stated in the introduction of the chapter, the interface of the end user was programmed in Python, with the usage of the TkInter library.

When initializing the Standard mode, the user is confronted with the following GUI:

## Chapter 4: Code Structure

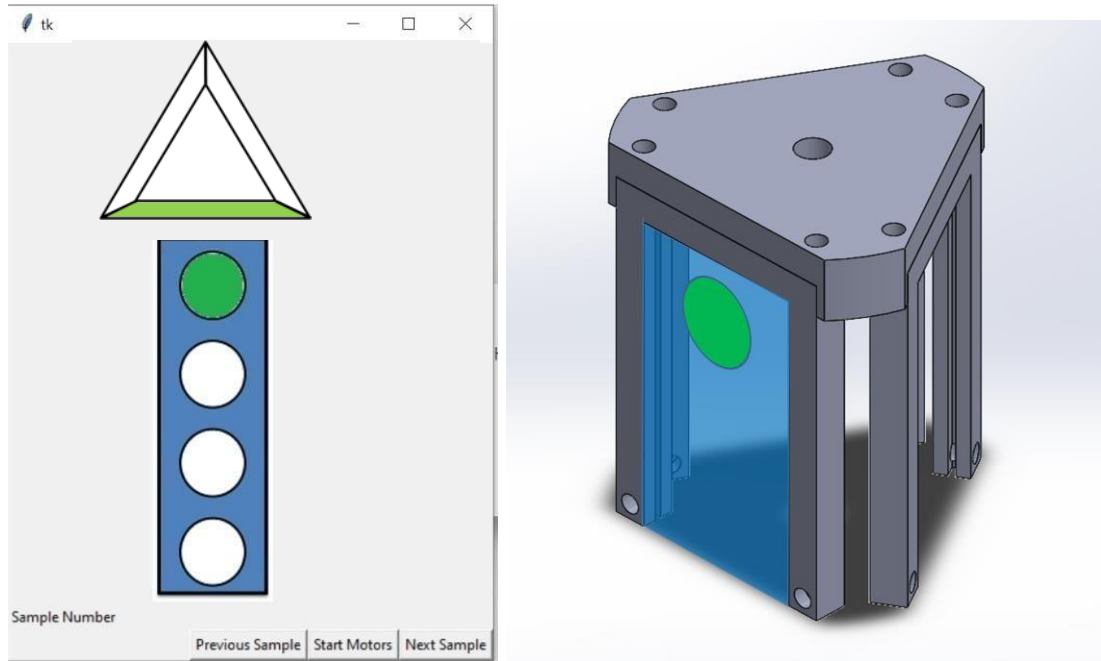


**Figure 4.2 - User GUI of the program (left) and SolidWorks 3D representation (right).**

When the Start button is pressed the Python connects to the Arduino and displays the current position of the sample holder being analyzed, this is represented with the green circle in the square at the bottom, and the face being analyzed represented in the pentagon at the top, a 3D representation of this is presented on the right of the image, blue being the face where the sample is located in the sample holder, and green being the position of the sample.

As the "next sample" button is pressed, the sample number goes up and the Python communicates to the Arduino to move the motors, the logic that the

## Chapter 4: Code Structure

---

Python program follows is displayed in the flowcharts bellow.

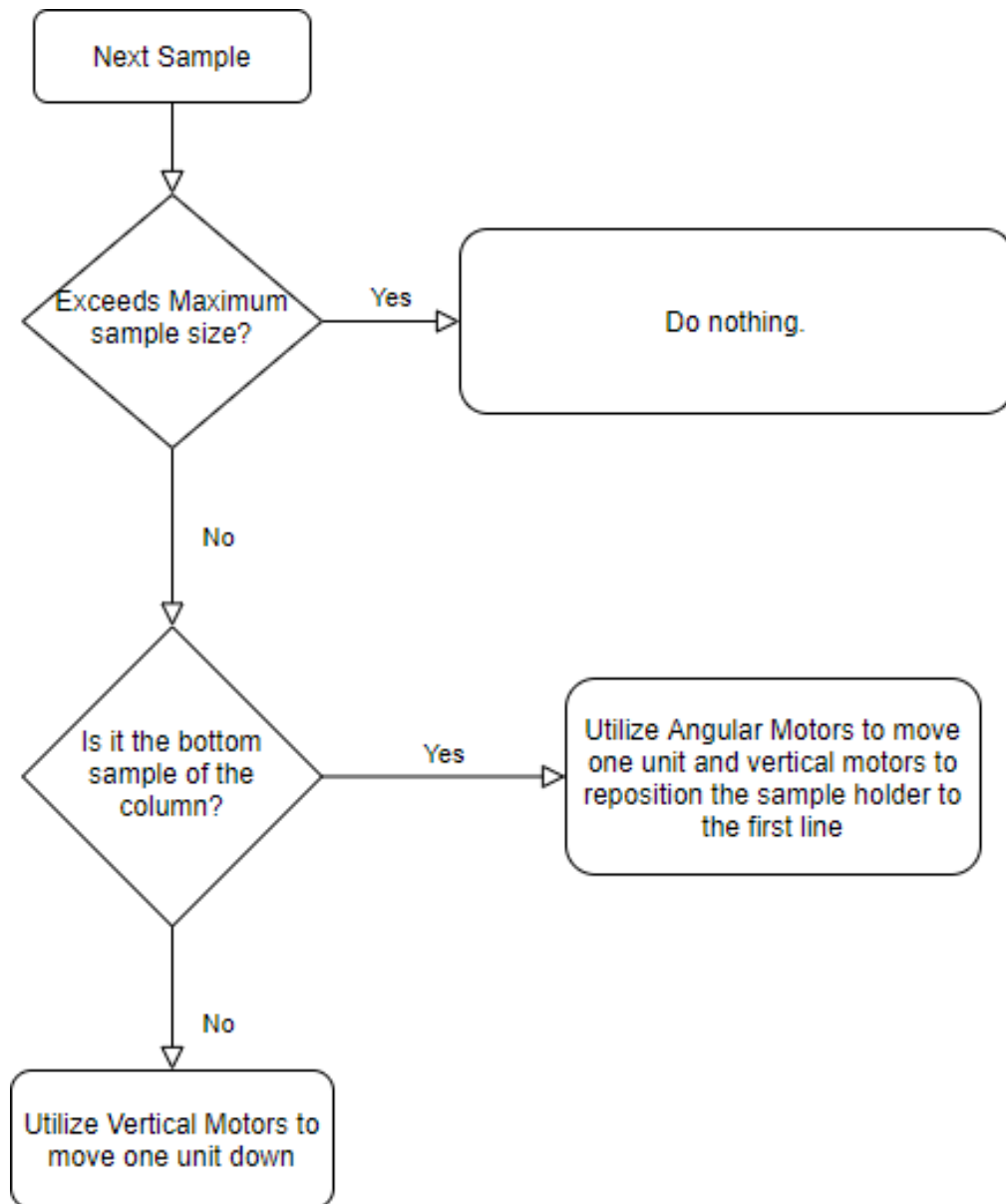


Figure 4.3(a) - Flowchart of the program for Next Sample

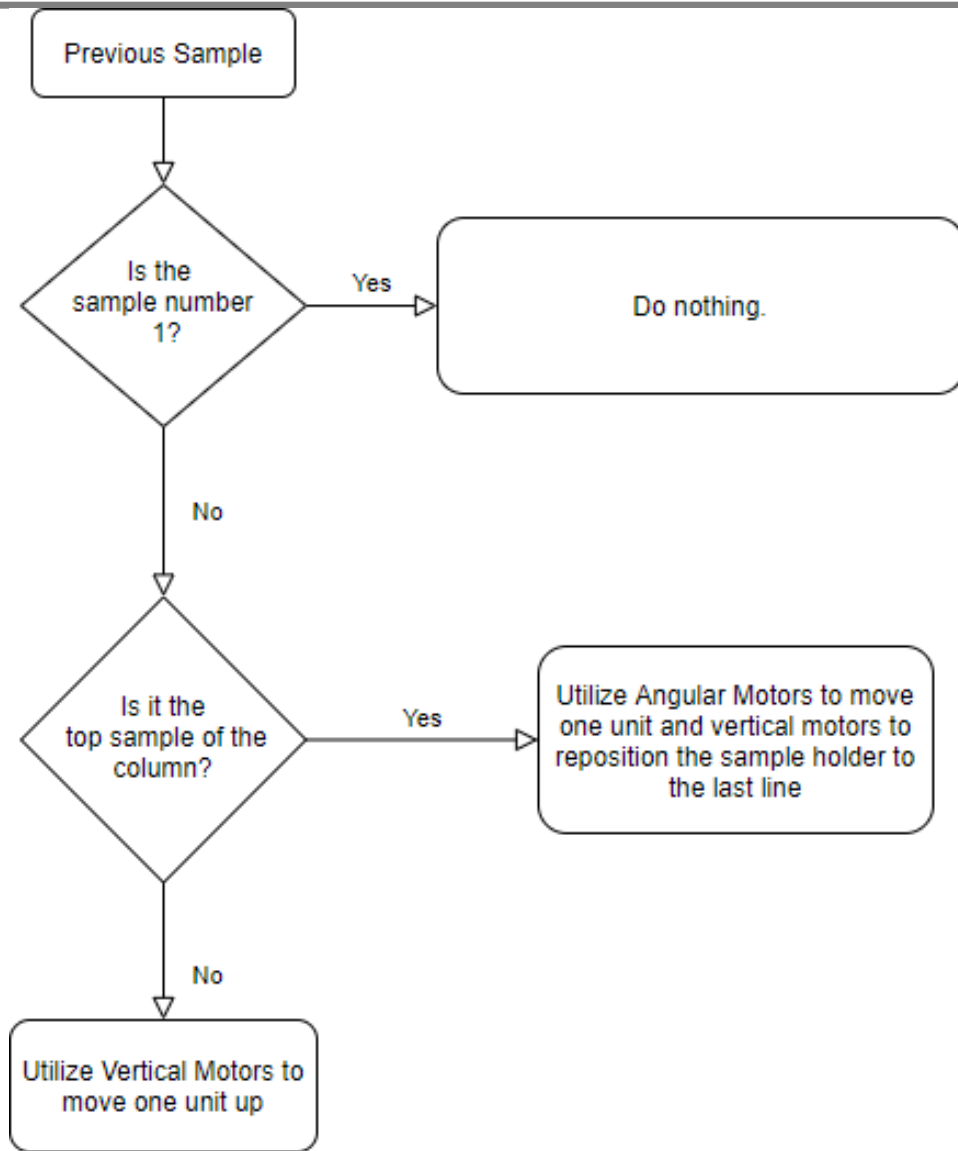


Figure 4.3(b) Flowchart of the program for Previous Sample

# Chapter 4: Code Structure

---

In the code and in the logic of the Flowchart above two types of motors are distinguished. The motors are the same model, the positioning of them and their connection to different parts of the system above the vacuum chamber is what will allow the sample holder to move either vertically, or to rotate.

## 4.3 Manual mode

The Manual Mode was made in case a future sample holder design is presented; this facilitates the incorporation of multiple sample holders into the same code.

In this mode the positioning of the samples is not fixed, so the user must manually insert the location of them, both its angular position as well as its vertical position.

When opening this mode, the user is presented with the following display:

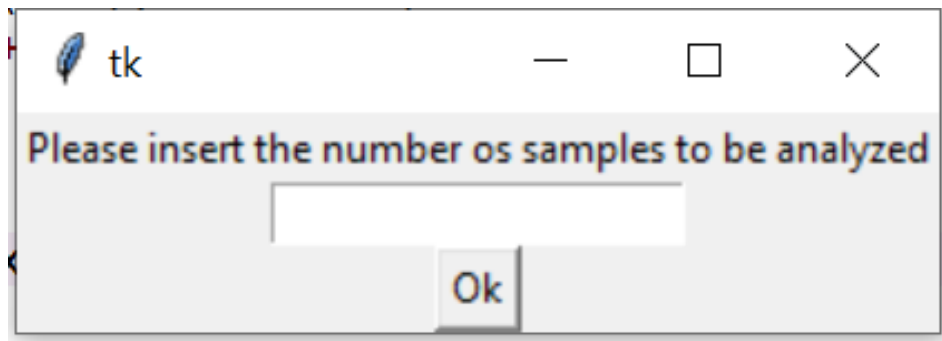
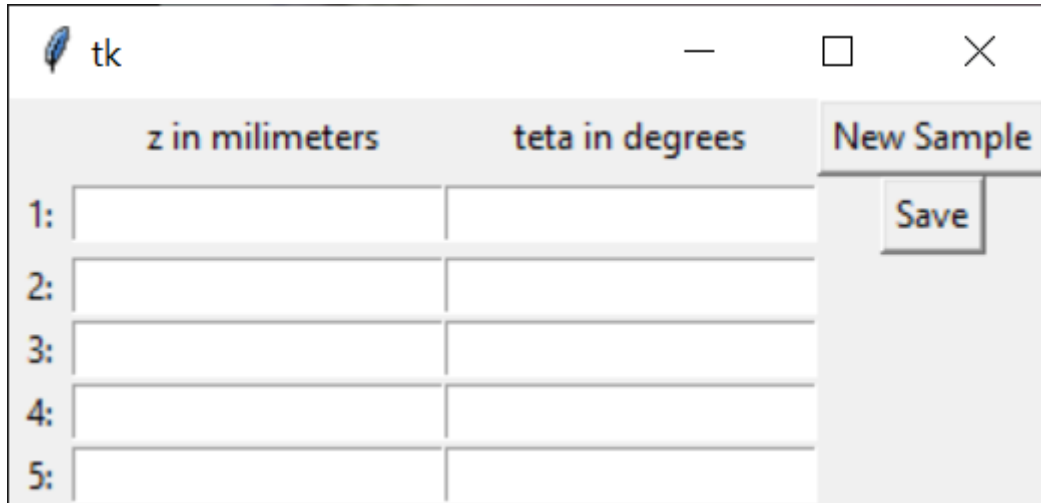


**Figure 4.4 - Initial display of the program.**

With this the user must insert the number of samples to analyze  
Having done that, a new menu appears as shown in Fig. 4.5 for an example of 5 samples chosen.

## Chapter 4: Code Structure



	z in millimeters	teta in degrees	New Sample
1:			Save
2:			
3:			
4:			
5:			

**Figure 4.5 - Secondary Display with 5 samples selected in the first display.**

The user fills all the boxes with the positions of the different samples; the program will store internally the locations of each sample and calculate the distance between each of the samples. For this calculation, the program considers the current position, the motor being utilized, and the final position the sample will be in.

# Chapter 4: Code Structure

Bellow a labeled version is presented, that explains each part of the UI.

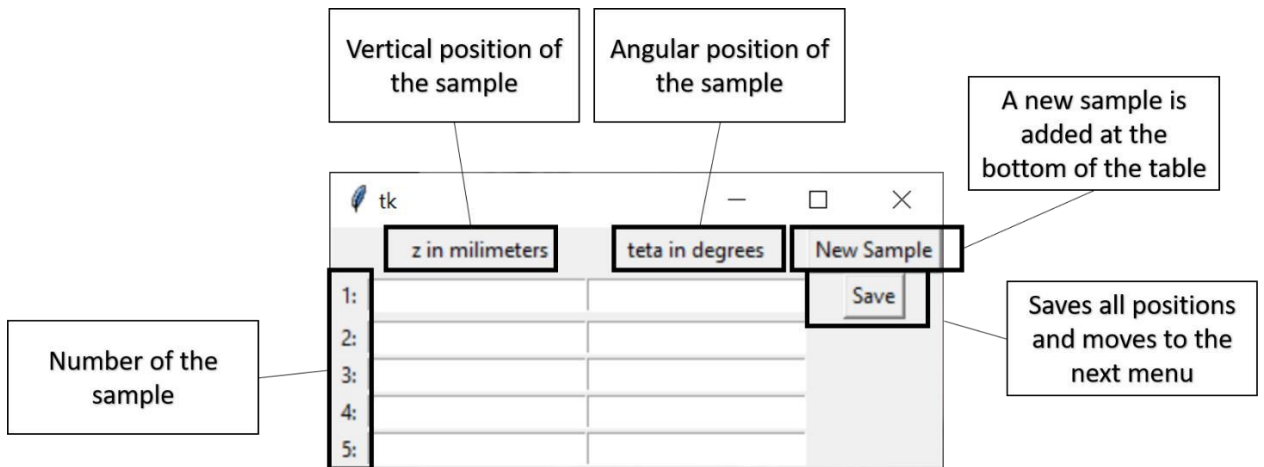


Figure 4.6 - Labeled version of Figure 4.5.

The vertical position of the sample refers to the position in the z axis where the sample is positioned (Fig 4.7 left); this field should be filled in units of millimeters. For the angular position, the user must fill it in degrees in accordance with (Fig 4.7 right – 0° stands for initial angular position).The number of the sample indicates the order that the program will position each sample into the array. New Sample adds a new row at the bottom of the UI if the introduction of a new sample is necessary.

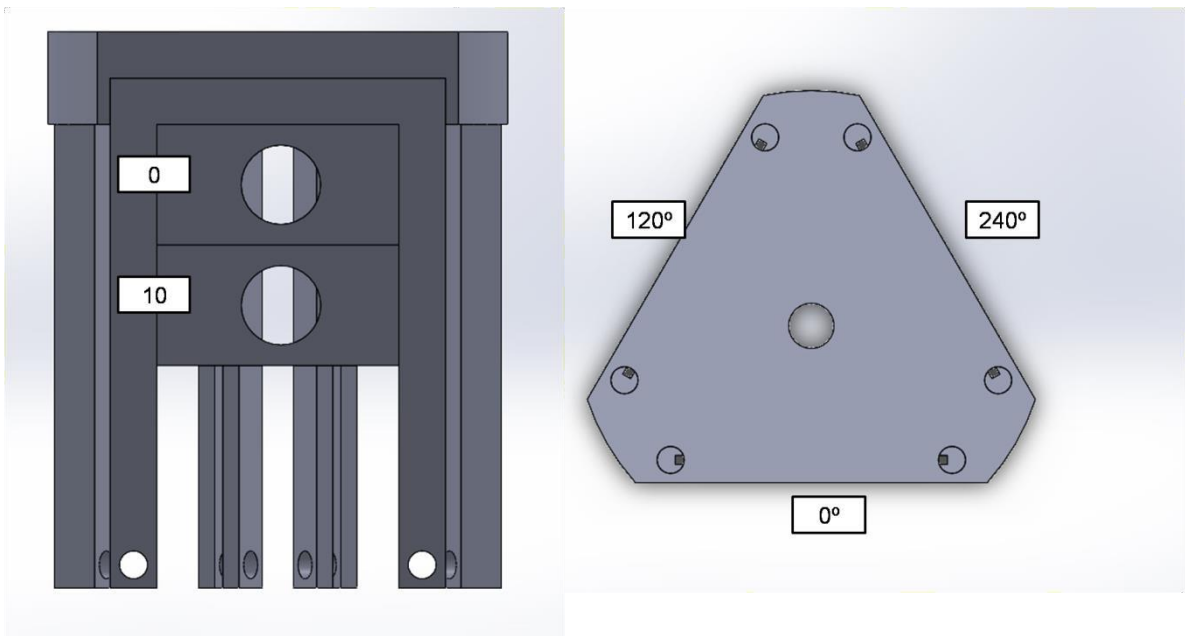
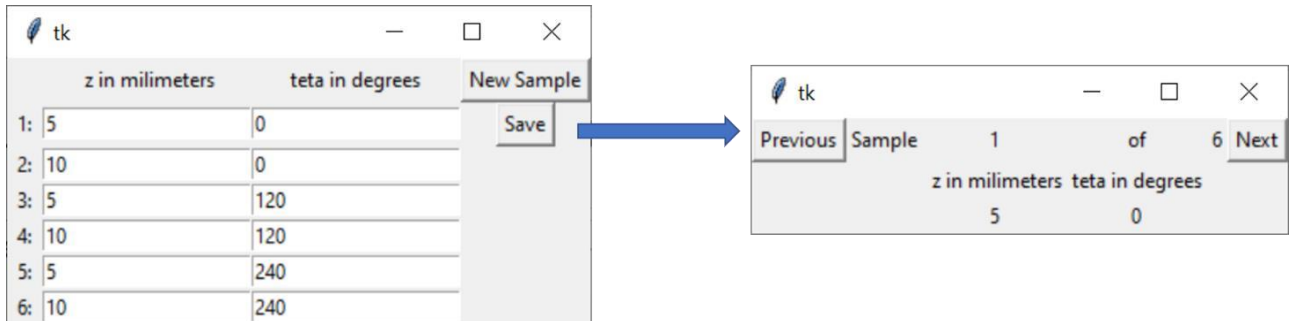


Figure 4.7 - Positioning considered by the program of vertical positions (left) and angular positions (right) as displayed in Figure 4.8.



# Chapter 4: Code Structure

Filling this menu and pressing “Save” will give you next menu, the program will import each filled cell into an array and do its calculations on the numbers filled.



**Figure 4.8 - Example of a filled UI (left) and first position of the sample (right).**

In this menu we can see the number of the sample being analyzed out of a total of samples and the current position of the sample being analyzed.

When the “Next” button is pressed, the program will communicate to the Arduino to move the motors to the next sample, same logic applies to the “Previous” button.

## 4.4 System connections

With the software part of the system explained, this subchapter is dedicated to the hardware part of the system, meaning the motor controller, the motors and the system positioned over the vacuum chamber.

### 4.1.1 Python to Arduino to Gecko drive to Motors

Python communicates to Arduino the user's commands, and the Arduino sends that information to the motor controller, model G540 4-AXIS DRIVE that will be referred to as Gecko from now on.

# Chapter 4: Code Structure

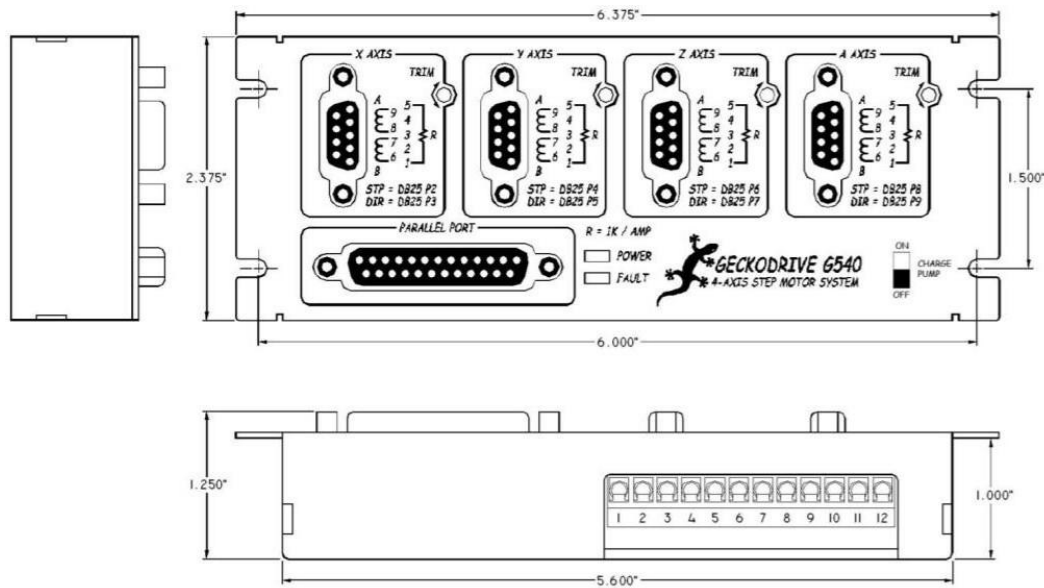


**Figure 4.9 - Gecko connections.**

The communication between the Python and the Arduino board are done utilizing a simple USB cable, this cable is also responsible for powering the Arduino.

The communication between the Arduino board and the Gecko is done via a DB-25 cable, the ends of the cable are welded into the Arduino board, and with this we can establish communication with the Gecko.

The order of the pins in the Gecko are important, below is a listing of each pin's function in the Gecko.

The first pin indicated the output, with this the Gecko can communicate with the Arduino any possible errors that occurred during the transferring of data between the two.

The step refers to the actual steps of the stepper motor, so 1 step would correspond to the motion of 1 step of the motor. The direction, much like the name indicates, is utilized for the direction of the motor, either going clockwise or counterclockwise. The GND is connected to the ground of the Arduino, so that everything stays on the same ground. Finally, the Gecko is connected to the motors utilizing DB-9 cables, the pins of these matter too.

Between pins 1 and 5 a resistor of 2.8 k $\Omega$  was connected, this provides the necessary current for the motors to function.

## Chapter 4: Code Structure

---

The equation to determine the resistance of the resistor is the following:

$$R = \frac{1 \text{ K}\Omega}{I}$$

Where R is the necessary resistance, and I is the current that the motor needs to function.

The Gecko is connected to a power source that provides the necessary power to move the motors.

## Summary and Final Remarks

### 5.1 Conclusions

The goal this project aimed to achieve was the construction of a new sample holder for the tandem accelerator tandem. Associated with this was the development of a new Faraday Cage, a new lid and the coding of both Arduino and Python.

The new triangular sample holder constructed out of aluminum has the capability of holding a maximum of fifteen samples, five on each side of the triangular holder. The sample holder is capable of slotting in the already present aluminum laminal sample holders, described in chapter 3.2.2.

The new lid constructed out of stainless steel has its tube to insert the new sample holder off-centered from the center of the chamber to allow the correct positioning of the samples when doing their analyses. The lid can also incorporate a BNC like the old one previously developed [1].

The new code was tested in the motors that will be incorporated in the feedthrough and the Two Stage Differentially Pumped Rotary Platform and is capable of utilizing multiple sample holders without editing the code itself.

The new Faraday Cage has the possibility of using the new sample holder, as well as the old sample holder by the usage of two different copper lids.

## 5.2 Future Prospects

With the finalization of this project some prospects for the code and parts can be presented. For starters since the code can introduce up to four motors, the possibility of moving the samples in two more degrees is possible. The sample holder developed during this project can only move the samples in two degrees of freedom, a vertical and a rotational, but the sample itself individually is always analyzed at a  $90^\circ$  angle with the beam, unfortunately the implementation of this new model will need the design and construction of a new sample holder. The code developed during this work can introduce up to 4 motors to the system, we also have a third and fourth motors ready to be implemented if necessary, with the proper welding into a DB-9 with the correct resistors to do so as well. Another idea proposed, was that of the motorized motion of the PIPS detectors inside the vacuum chamber, to note, the present code does not take into account the motion of these.

# References

- [1] R. Mateus, "Recolha automática de aerossóis e sua análise por técnicas analíticas nucleares," Ph.D. Dissertation, Faculdade de Ciências e Tecnologia, Universidade Nova de Lisboa, Lisboa, PT, 2003.
- [2] K.Dias " Determinação da distribuição de flúor em esmalte dentário" M.S. Thesis, Faculdade de Ciências e Tecnologia, Universidade Nova de Lisboa, Lisboa, PT, 2017.
- [3] M. Fonseca, "Análise de elementos leves por reacções nucleares com produção de radiação 84 gama," Ph.D. Dissertation, Faculdade de Ciências e Tecnologia, Universidade Nova de Lisboa, Lisboa, PT, 2010.
- [4] Schieck, H. P. (2015). Key nuclear reaction experiments: Discoveries and consequences. Bristol: IOP
- [5] L.D. LANDAU, E.M. LIFSHITZ, in Quantum Mechanics (Third Edition), 1977
- [6] E., R. (1911). The Scattering of  $\alpha$  and  $\beta$  rays by Matter and the Structure of the Atom.Philosophical Magazine.
- [7] Syed Naeem Ahmed, in Physics and Engineering of Radiation Detection (Second Edition), 2015].
- [8] Henderson, H. (2014). *Nuclear power: A reference handbook*. Santa Barbara

- [9] Michael F. L'Annunziata, in *Radioactivity (Second Edition)*, 2016
- [10] GREGORY R. CHOPPIN, ... JAN RYDBERG, in *Radiochemistry and Nuclear Chemistry (Third Edition)*, 2002
- [11] Arthur Beiser (2003). "Chapter 12: Nuclear Transformations
- [12] Taylor, R. J., Baker, D. R., & Ikezi, H. (1970). Observation of Collisionless Electrostatic Shocks. *Physical Review Letters*, 24(5), 206-209
- [13] W. H. Bragg M.A. & R. Kleeman B.Sc. (1905) XXXIX. On the  $\alpha$  particles of radium, and their loss of range in passing through various atoms and molecules, *The London, Edinburgh, and Dublin Philosophical Magazine and Journal of Science*, 10:57, 318-340
- [14] Henderson, H. (2014). *Nuclear power: A reference handbook*. Santa Barbara, CA: ABC-CLIO.
- [15] Gümüş, H. (2005). Simple stopping power formula for low and intermediate energy electrons. *Radiation Physics and Chemistry*, 72(1), 7-12.
- [16] Charles J. Fraser, in *Mechanical Engineer's Reference Book (Twelfth Edition)*, 1994
- [17] Ruffer, A. C. (1998). Nuclear inelastic scattering. *Hyperfine Interactions*, 59–79.
- [18] TM, K. (1993). *Física Nuclear*. Lisboa: Fundação Calouste Gulbenkian.
- [19] (2007) Rutherford Backscattering Spectroscopy. In: *Atomic and Nuclear Analytical Methods*. Springer, Berlin, Heidelberg. (Barfoot 1986)

- [20] Faraday Cage - MagLab. (n.d.). Retrieved December 10, 2020, from <https://nationalmaglab.org/about/around-the-lab/what-the/faraday-cage>
- [21] H. F. Luis, "Study of nuclear reactions relevant for astrophysics by Micro-AMS," Ph.D. Dissertation, Faculdade de Ciências e Tecnologia, Universidade Nova de Lisboa, Lisboa, PT, 2013
- [22] Differentially Pumped Rotary Platform (DPRP) Instructions. (n.d.). Manual. Retrieved December 10, 2020, from [https://www.lesker.com/newweb/sample\\_manipulation/pdf/kjlc-dprp-manual.pdf](https://www.lesker.com/newweb/sample_manipulation/pdf/kjlc-dprp-manual.pdf)<https://www.lewvac.co.uk/product/two-stage-differentially-pumped-rotary-platforms/>
- [23] Krane, K. S., & Krane, K. S. (1989). *Problem solutions for Introductory nuclear physics*. New York: Wiley.
- [24] H. Silva, "Elastic scattering of protons and oxygen ions from light nuclei," Ph.D. Dissertation, Faculdade de Ciências e Tecnologia, Universidade Nova de Lisboa, Lisboa, PT, 2018.
- [25] Walter Loveland, in *Encyclopedia of Physical Science and Technology* (Third Edition), 2003
- [26] Rutherford Scattering. (n.d.). Retrieved December 18, 2020, from <http://hyperphysics.phy-astr.gsu.edu/hbase/rutsca.html>
- [27] Raich, U. (2016). *Accelerators for pedestrians*. Lecture presented in Kigali, Rwanda





# Appendix

## 7.1 Code

### 7.1.1 Python

```
Arduinofromtkinterimport*

importtkinterastk
fromfunctoolsimportpartial
importserial
importtime
importpyfirmata

stepangle=1.8

count=1
cells=4
arduinoData=serial.Serial('COM3',9600)
Stepmotorx=300#nr de passos para uma volta no motor x
Stepmotory=300#nr de passos para uma volta no motor y

SizeRotor=300#nr de passos para dar uma volta do bellow angular
SizeBello=300#nr de passos para dar uma volta no bellowverical

currentsample=0

#
#meter posição inicial do motor
#meter posição exata em termos de passos.
# o geckoso precisa de 2 por

defSteps(passosx,dirx,passosy,diry,passosz,dirz,passoso, diro):

if(type(passosx)==type(12)):
    PASSOSX =passosx
else:
    PASSOSX =0

if(type(dirx)==type(12)):
    DIRX =dirx
else:
    DIRX =0

if(type(passosy)==type(12)):
    PASSOSY =passosy
else:
    PASSOSY =0

if(type(diry)==type(12)):
    DIRY =diry
else:
    DIRY =0

if(type(passosz)==type(12)):
    PASSOSZ =passosz
```

```

else:
    PASSOSZ =0

if (type (dirz)==type (12)) :
    DIRZ =dirz
else:
    DIRZ =0

if (type (passoso)==type (12)) :
    PASSOSO =passoso
else:
    PASSOSO =0

if (type (diro)==type (12)) :
    DIRO = diro
else:
    DIRO =0

    INFO =[PASSOSX, DIRX, PASSOSY, DIRY, PASSOSZ, DIRZ, PASSOSO, DIRO]
#Serial.write (buf, INFO)
print (INFO)

for i in range (8) :
    Value =chr (INFO[i])
    arduinoData.write (Value.encode ())
    print (INFO[i])

def Manual () :

def Number () :

    samples =int (e1.get ())

Manual.destroy ()
    Samples =Tk ()
def on_closing () :
if messagebox.askokcancel ("Quit", "Do you want to quit?") :
Samples.destroy ()
arduinoData.close ()
#arrays teta e z
Samples.entries=[]
Samples.tetas=[]
arrayteta=[]
arrayz=[]
    number =1
i=0

#defenir labels
number_label=Label (Samples, text =("Sample"))

    number =Label (Samples, text = number)

number_label_of=Label (Samples, text =("of"))

```

```

        samples1 =Label(Samples, text = samples)

defNew():
    n =len(Samples.entries)
    Samples.entries.append(tk.Entry(Samples))
    Samples.tetas.append(tk.Entry(Samples))
    tk.Label(Samples,text="%2d: "%(n+1)).grid(row=(n+1),column=0)
    Samples.entries[n].grid(row=(n+1),column=1)
    Samples.tetas[n].grid(row=(n+1),column=2)

New_sample= Button(Samples, text ="New Sample", command = New )

zlabel=Label(Samples, text =" z in millimeters")
tetalabel=Label(Samples, text ="teta in degrees")

Samples.protocol("WM_DELETE_WINDOW",on_closing)

if (type(samples)==type(12)):

for n inrange(samples):

    Samples.entries.append(tk.Entry(Samples))

    Samples.tetas.append(tk.Entry(Samples))
    tk.Label(Samples,text="%2d: "%(n+1)).grid(row=(n+1),column=0)
    Samples.entries[n].grid(row=(n+1),column=1)
    Samples.tetas[n].grid(row=(n+1),column=2)

if (type(samples)!=type(12)):
    print("not int")

defSave():
    ArrayTeta=[]
    ArrayZ=[]
    N_samples=len(Samples.tetas)

    foriinrange(N_samples):
        ArrayTeta.append(Samples.tetas[i].get())
        ArrayZ.append(Samples.entries[i].get())

    Samples.destroy()
        Saved =Tk()

defNEXT():
globalcurrentsample

ifcurrentsample!=N_samples-1:
    currentsample=currentsample+1
    tetan=ArrayTeta[currentsample]
    zetan=ArrayZ[currentsample]

```

```

        TETA =Label(Saved, text =tetan)
        Z =Label(Saved, text =zetan)
TETA.grid(row=2, column =3)
Z.grid(row =2, column =2)
Label_nr= Label(Saved, text =currentsample+1)
Label_nr.grid(row=0, column =2)

if(currentsample==0):
passosz=int(ArrayZ[currentsample])
passosteta=int(ArrayTeta[currentsample])
else:
passosz=int(ArrayZ[currentsample])-int(ArrayZ[currentsample-1])
passosteta=int(ArrayTeta[currentsample])-int(ArrayTeta[currentsample-1])

#motorz = 1
#motorteta = 2

Steps(passosz,1,passosteta,1,1,1,1,1)

defPREVIOUS():
globalcurrentsample

ifcurrentsample>0:

currentsample=currentsample-1
tetan=ArrayTeta[currentsample]
zetan=ArrayZ[currentsample]
        TETA =Label(Saved, text =tetan)
        Z =Label(Saved, text =zetan)
TETA.grid(row=2, column =3)
Z.grid(row =2, column =2)
Label_nr=Label(Saved, text =currentsample+1)
Label_nr.grid(row=0, column =2)

if(currentsample==0):
passosz=int(ArrayZ[currentsample])
passosteta=int(ArrayTeta[currentsample])
else:
passosz=int(ArrayZ[currentsample])-int(ArrayZ[currentsample-1])
passosteta=int(ArrayTeta[currentsample])-int(ArrayTeta[currentsample-1])

#motorz = 1
#motorteta = 2

Steps(passosz,1,passosteta,1,1,1,1,1)

Label_Sample=Label(Saved, text ="Sample")
Label_of=Label(Saved, text ="of")
Label_total=Label(Saved, text =N_samples)
        Next =Button(Saved, text ="Next", command = NEXT)
        Previous =Button(Saved, text ="Previous", command =
PREVIOUS)

```

```

zlabel=Label(Saved, text =" z in milimeters")
tetalabel=Label(Saved, text ="teta in degrees")
tetan=ArrayTeta[0]
zetan=ArrayZ[0]
        TETA =Label(Saved, text =tetan)
        Z =Label(Saved, text =zetan)
TETA.grid(row=2, column =3)
Z.grid(row =2, column =2)

Label_nr=Label(Saved, text =1)
Label_nr.grid(row=0, column =2)

zlabel.grid(row =1, column =2)
tetalabel.grid(row =1, column =3)

Label_Sample.grid(row =0, column =1)
Label_of.grid(row =0, column =3)
Label_total.grid(row =0, column =4)
Next.grid(row =0,column=5)
Previous.grid(row =0, column =0)
passosz=int(ArrayZ[currentsample])
passosteta=int(ArrayTeta[currentsample])

#motorz = 1
#motorteta = 2

Steps(passosz,1,passosteta,1,1,1,1,1)
#posicoes
zlabel.grid(row =0, column =1)
tetalabel.grid(row =0, column =2)
New_sample.grid(row=0, column =3)
        Save = Button(Samples, text ="Save", command = Save )
Save.grid(row=1,column=3)

inicial.destroy()
        Manual =Tk()
# Cenas na janela
labell =Label(Manual, text ="Please insert the number os samples to be
analyzed")
        e1 =tk.Entry(Manual)

botaomanual=Button(Manual, text ="Ok", command = Number)

        labell.grid(row=0, column=0)
        e1.grid(row=1, column=0)
botaomanual.grid(row =2, column =0)

```

```

defStandart():
    inicial.destroy()

    root =Tk()

defMudaQuadradoN():
    print("quadrado inteiro Next")
    Steps(10,1,10,1,1,1,1,1)

defMudaAmostraN():
    print("amostra next")
    Steps(10,1,10,1,0,0,0,0)

defMudaQuadradoP():
    print("quadrado P")
    Steps(10,1,10,1,0,0,0,0)

defMudaAmostraP():
    print("amotra p")
    Steps(10,1,10,1,0,0,0,0)

defon_closing():
    ifmessagebox.askokcancel("Quit","Do you want to quit?"):
        root.destroy()
        arduinoData.close()

root.protocol("WM_DELETE_WINDOW",on_closing)

#movimento
defGoright():
    global count
    if(count >1):
        count = count -1
        count1.configure(text=f' {count} ')
    Testesdeimagem()
    if(count%4==0):
        MudaQuadradoP()

    else:
        MudaAmostraP()
        print("Motor moving to the right")

    else:
        print("no more samples")

defGoleft():

```

```

global count
if(count <20):
print("Motor moving to the left")

        count = count +1
        count1.configure(text=f' {count} ')
Testesdeimagem()
if(count %4==1):
MudaQuadradoN()
else:
MudaAmostraN()

else:print("no more samples")

```

```
defStart():
```

```
print("Start your engines")
```

```
global count
```

```
count =1
```

```
count1.configure(text=f' {count} ')

```

```
Testesdeimagem()
```

```
defTestesdeimagem():
```

```
if count <5and count >0:
```

```
pentagono_1 =PhotoImage(file ="pentagono1.png")
```

```
pentagono1 =Label(root,image= pentagono_1)
```

```
pentagono1.image = pentagono_1
```

```
if count%4==1:
```

```
quadrado_1 =PhotoImage(file ="quadrado1.png")
```

```
quadrado1 =Label(root,image= quadrado_1)
```

```
quadrado1.image = quadrado_1
```

```
if count%4==2:
```

```
quadrado_1=PhotoImage(file ="quadrado2.png")
```

```
quadrado1=Label(root,image= quadrado_1)
```

```
quadrado1.image=quadrado_1
```

```
if count%4==3:
```

```
quadrado_1=PhotoImage(file ="quadrado3.png")
```

```
quadrado1=Label(root,image= quadrado_1)
```

```
quadrado1.image=quadrado_1
```

```
if count%4==0:
```

```
quadrado_1=PhotoImage(file ="quadrado4.png")
```

```
quadrado1=Label(root,image= quadrado_1)
```

```
quadrado1.image=quadrado_1
```

```
if count <9and count >4:
```



```

pentagono_1 =PhotoImage(file ="pentagono2.png")
    pentagono1 =Label(root,image= pentagono_1)
    pentagono1.image = pentagono_1
if count%4==1:
    quadrado_1 =PhotoImage(file ="quadrado1.png")
    quadrado1 =Label(root,image= quadrado_1)
    quadrado1.image = quadrado_1
if count%4==2:
    quadrado_1=PhotoImage(file ="quadrado2.png")
    quadrado1=Label(root,image= quadrado_1)
    quadrado1.image=quadrado_1

if count%4==3:
    quadrado_1=PhotoImage(file ="quadrado3.png")
    quadrado1=Label(root,image= quadrado_1)
    quadrado1.image=quadrado_1

if count%4==0:
    quadrado_1=PhotoImage(file ="quadrado4.png")
    quadrado1=Label(root,image= quadrado_1)
quadrado1.image=quadrado_1

if count <13and count >8:
pentagono_1 =PhotoImage(file ="pentagono3.png")
    pentagono1 =Label(root,image= pentagono_1)
    pentagono1.image = pentagono_1
if count%4==1:
    quadrado_1 =PhotoImage(file ="quadrado1.png")
    quadrado1 =Label(root,image= quadrado_1)
    quadrado1.image = quadrado_1
if count%4==2:
    quadrado_1=PhotoImage(file ="quadrado2.png")
    quadrado1=Label(root,image= quadrado_1)
    quadrado1.image=quadrado_1

if count%4==3:
    quadrado_1=PhotoImage(file ="quadrado3.png")
    quadrado1=Label(root,image= quadrado_1)
    quadrado1.image=quadrado_1

if count%4==0:
    quadrado_1=PhotoImage(file ="quadrado4.png")
    quadrado1=Label(root,image= quadrado_1)
quadrado1.image=quadrado_1
if count <17and count >12:
pentagono_1 =PhotoImage(file ="pentagono4.png")
    pentagono1 =Label(root,image= pentagono_1)
    pentagono1.image = pentagono_1
if count%4==1:
    quadrado_1 =PhotoImage(file ="quadrado1.png")
    quadrado1 =Label(root,image= quadrado_1)
    quadrado1.image = quadrado_1
if count%4==2:
    quadrado_1=PhotoImage(file ="quadrado2.png")
    quadrado1=Label(root,image= quadrado_1)
    quadrado1.image=quadrado_1

if count%4==3:
    quadrado_1=PhotoImage(file ="quadrado3.png")

```

```

        quadrado1=Label(root,image= quadrado_1)
        quadrado1.image=quadrado_1

if count%4==0:
    quadrado_1=PhotoImage(file ="quadrado4.png")
    quadrado1=Label(root,image= quadrado_1)
quadrado1.image=quadrado_1
if count <21and count >16:

pentagono_1 =PhotoImage(file ="pentagono5.png")
    pentagono1 =Label(root,image= pentagono_1)
    pentagono1.image = pentagono_1

if count%4==1:
    quadrado_1 =PhotoImage(file ="quadrado1.png")
    quadrado1 =Label(root,image= quadrado_1)
    quadrado1.image = quadrado_1

if count%4==2:
    quadrado_1=PhotoImage(file ="quadrado2.png")
    quadrado1=Label(root,image= quadrado_1)
    quadrado1.image=quadrado_1

if count%4==3:
    quadrado_1=PhotoImage(file ="quadrado3.png")
    quadrado1=Label(root,image= quadrado_1)
    quadrado1.image=quadrado_1

if count%4==0:
    quadrado_1=PhotoImage(file ="quadrado4.png")
    quadrado1=Label(root,image= quadrado_1)
    quadrado1.image=quadrado_1
    pentagono1.grid(row=0,column=1)

    quadrado1.grid(row=1,column=1)
#definir as coisas na GUI

label1 =Label(root, text ="Total Samples Analyzed")
    label2 =Label(root, text ="Total Time Elapsed")
    label3 =Label(root, text ="Time Elapsed on Current Sample")
    label4 =Label(root, text ="Sample Number")
    count1 = Label(root)

    button1 =Button(root, text ="Previous Sample", command =Goright)
buttonStart=Button(root, text ="Start Motors", command = Start)

    button2 =Button(root, text ="Next Sample", command =Goleft)

#Sugestoes do Norberto
    button3 =Button(root, text ="Manual")
    button4 =Button(root, text ="Standard Sample")

#posicionamento das coisas na GUI
#label1.grid(row=0, column = 0, sticky = W)
#label2.grid(row=1, column = 0, sticky = W)
#label3.grid(row=2, column = 0, sticky = W)
    label4.grid(row=3, column =0, sticky = W)
    count1.grid(row=3, column =1)

    button1.grid(row =4, column =1, sticky = E)

```

```
buttonStart.grid(row =4, column =2)
    button2.grid(row =4, column =3)
```

```
Testesdeimagem()
root.mainloop()
```

```
inicial =Tk()
#defenir manual e standart
buttonstandart=Button(inicial, text ="Standard", command =Standart)
botaomanual=Button(inicial, text ="Manual", command = Manual)
#posiçoes
buttonstandart.grid(row =1, column =1, sticky = E ,ipadx=100,ipady=50)
botaomanual.grid(row =1, column =2, sticky = E,ipadx=100,ipady=50)
```

```
inicial.mainloop()
```

### 7.1.1.1 Arduino

```
#include <Wire.h>
#include <Firmata.h>
```

```
int incomingByte; // for incoming serial data
byte available = -1;
int counter = 0;
// usar o write emvez do step.
```

```
void setup() {
Serial.begin(9600);
pinMode(LED_BUILTIN, OUTPUT);
```

```
for(int i=1; i<=15; i++)
{
pinMode(i, OUTPUT);
}
}
```

```
void loop() {
```

```
digitalWrite(1, LOW);
if (counter == 8){
digitalWrite(13, HIGH);
counter =0;}
if (Serial.available() > -1){
int temp = Serial.read();
if (temp > -1){

incomingByte = temp;
available = Serial.available();
digitalWrite(12, HIGH);
delay(100);
```

```

digitalWrite(12,LOW);
    counter++;
}
}

// Steps Motor 1
if (counter == 1){
for(int i = 0; i<incomingByte; i++)
{
digitalWrite(3, HIGH);    // turn the LED on (HIGH is the voltage
level)
delay(100);                // wait for a second
digitalWrite(3, LOW);    // turn the LED off by making the voltage LOW
delay(100);

}}

// Direção Motor 1
if (counter == 2){
digitalWrite(4, HIGH);

}

// Steps Motor 2
if (counter == 3){
for(int i = 0; i<incomingByte/10; i++)
{
digitalWrite(5, HIGH);    // turn the LED on (HIGH is the voltage
level)
delay(10);                // wait for a second
digitalWrite(5, LOW);    // turn the LED off by making the voltage LOW
delay(10);

}}

// Direção Motor 2
if (counter == 4){

digitalWrite(6, HIGH);
}

// Steps Motor 3
if (counter == 5){
for(int i = 0; i<incomingByte/10; i++)
{
digitalWrite(7, HIGH);    // turn the LED on (HIGH is the voltage
level)
delay(100);                // wait for a second
digitalWrite(7, LOW);    // turn the LED off by making the voltage LOW
delay(100);

}}

// Direção Motor 3
if (counter == 6){

digitalWrite(8, HIGH);
delay (100);
}
}

```

```
// Steps Motor 4
if (counter == 7){
for(int i = 0; i<incomingByte/10; i++)
{
digitalWrite(9, HIGH); // turn the LED on (HIGH is the voltage
level)
delay(100); // wait for a second
digitalWrite(9, LOW); // turn the LED off by making the voltage LOW
delay(100);

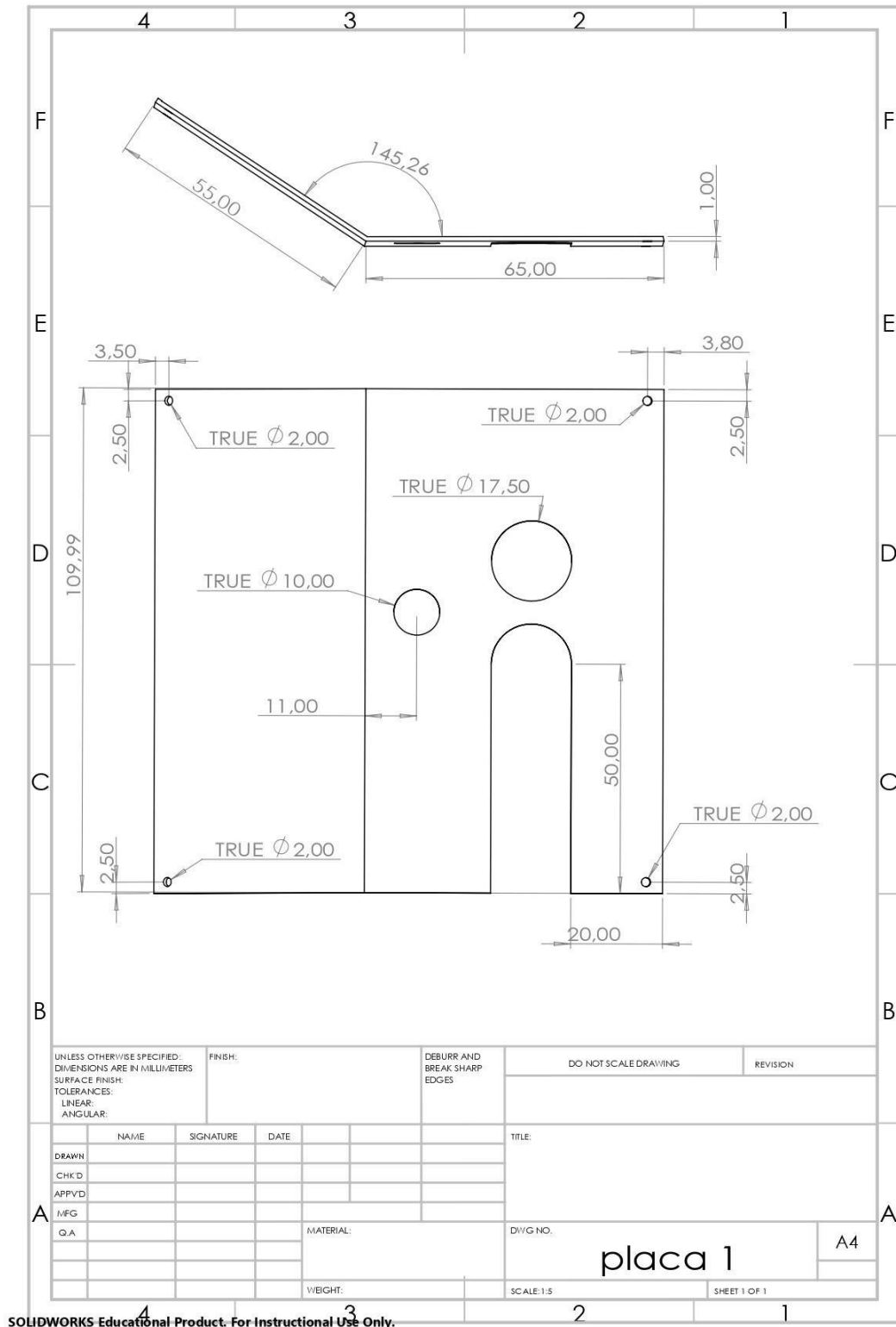
}}

// Direção Motor 4
if (counter == 8){

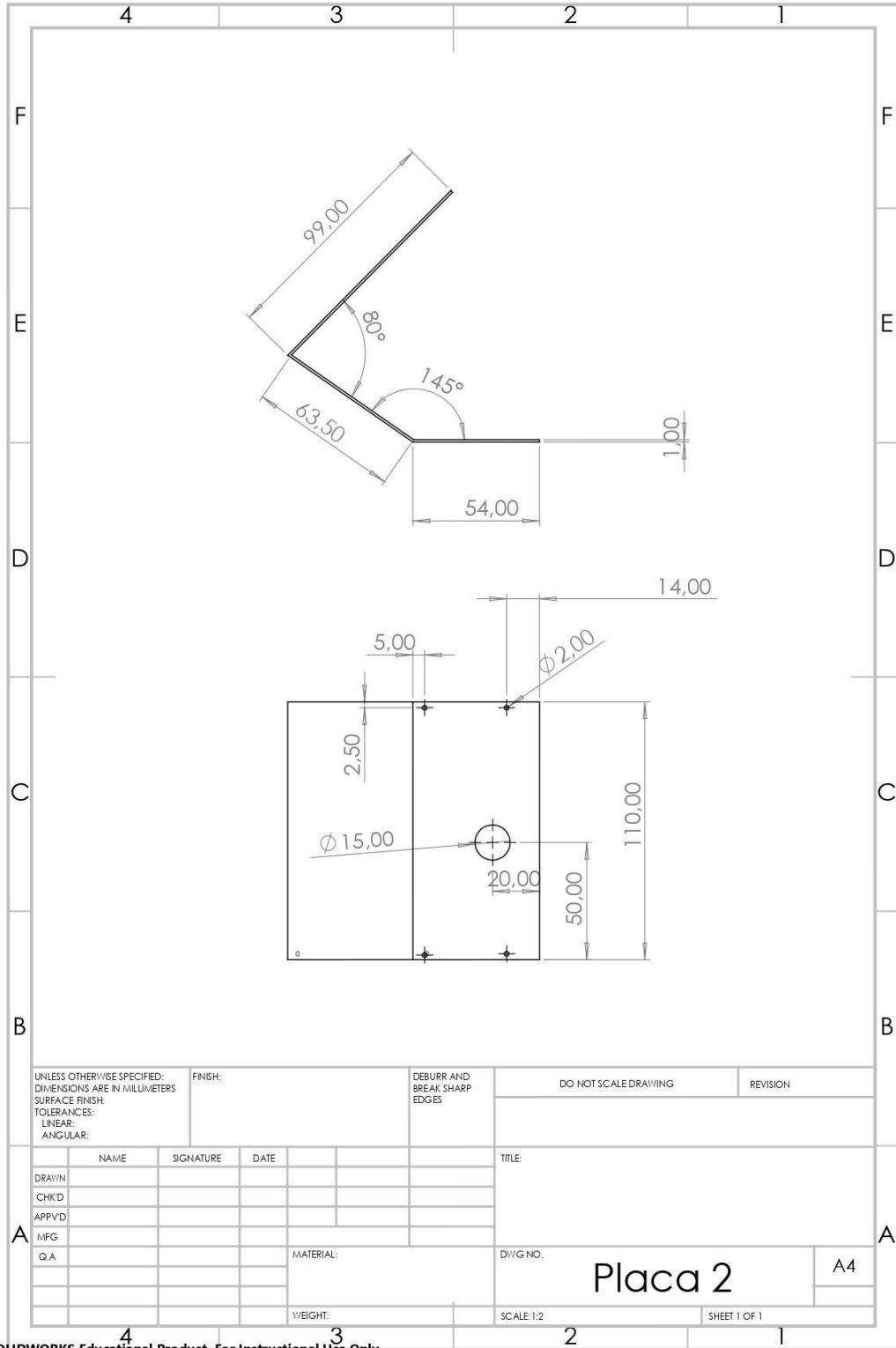
digitalWrite(10, HIGH);
delay (100);
```

## 7.2 Blueprints

### 7.2.1 Faraday Cage

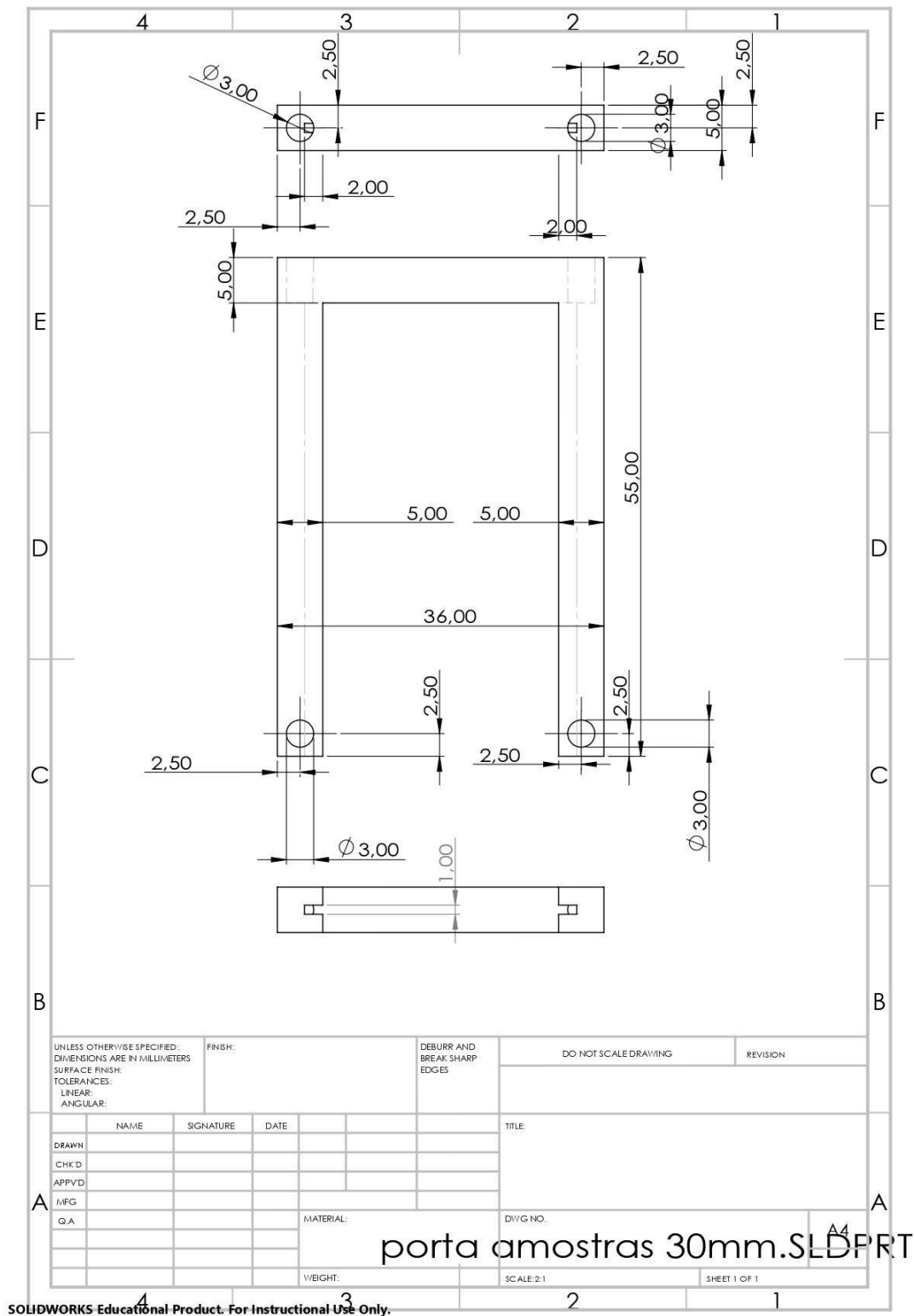


SOLIDWORKS Educational Product. For Instructional Use Only.



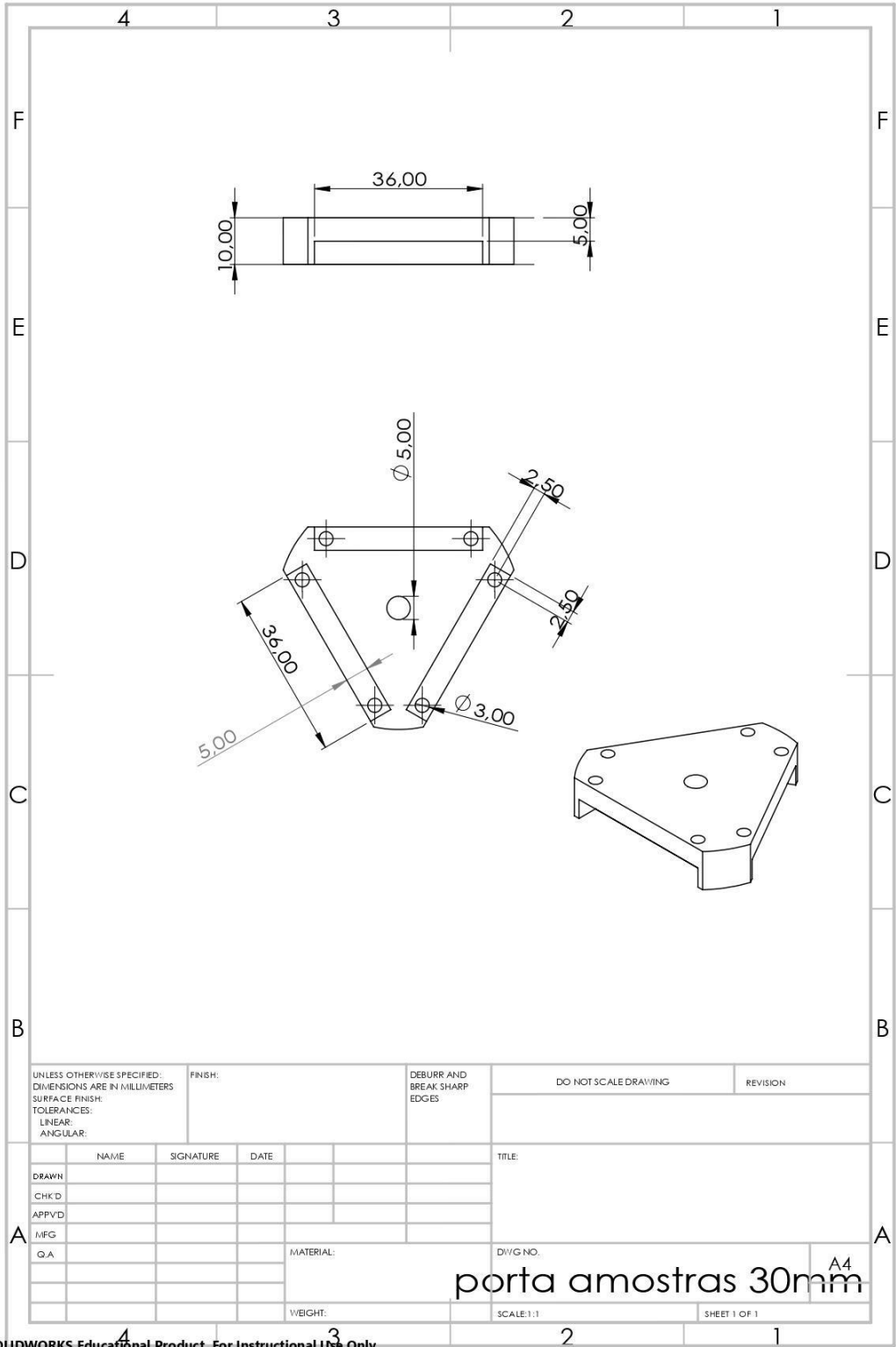
SOLIDWORKS Educational Product. For Instructional Use Only.

## 7.2.2 Sample Holder



SOLIDWORKS Educational Product. For Instructional Use Only.

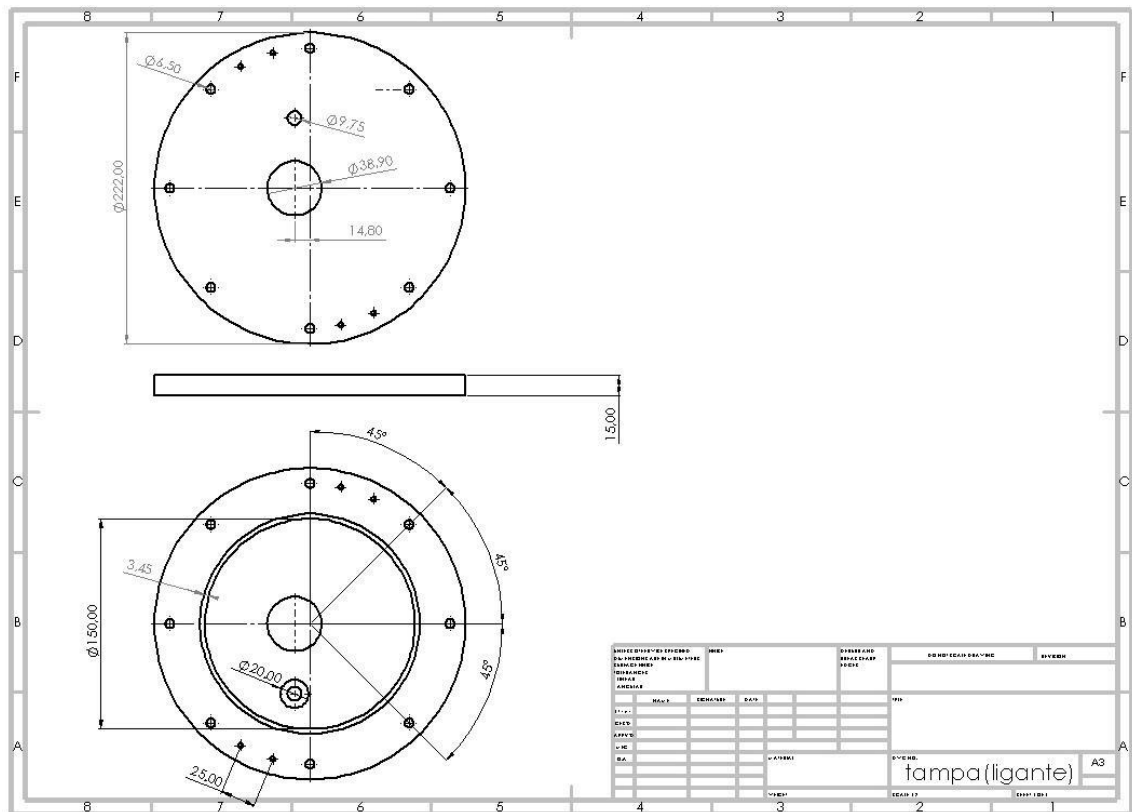




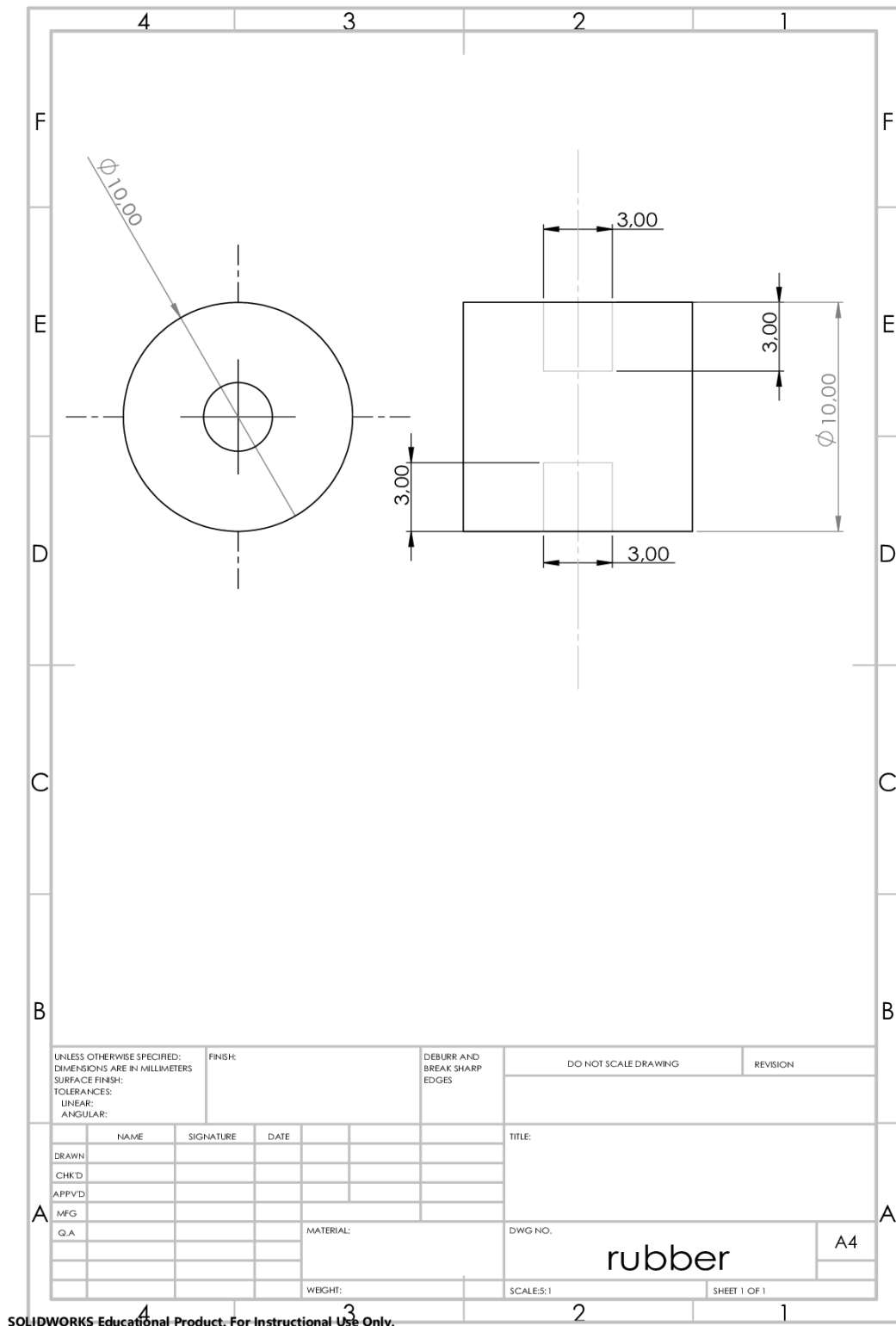
UNLESS OTHERWISE SPECIFIED: DIMENSIONS ARE IN MILLIMETERS SURFACE FINISH: TOLERANCES: LINEAR: ANGULAR:		FINISH:	DEBURR AND BREAK SHARP EDGES	DO NOT SCALE DRAWING	REVISION
NAME	SIGNATURE	DATE		TITLE:	
DRAWN					
CHK'D					
APP'VD					
MFG					
Q.A			MATERIAL:	DWG NO.	
			WEIGHT:	SCALE: 1:1	SHEET 1 OF 1

porta amostras 30mm A4

### 7.2.3 Lid

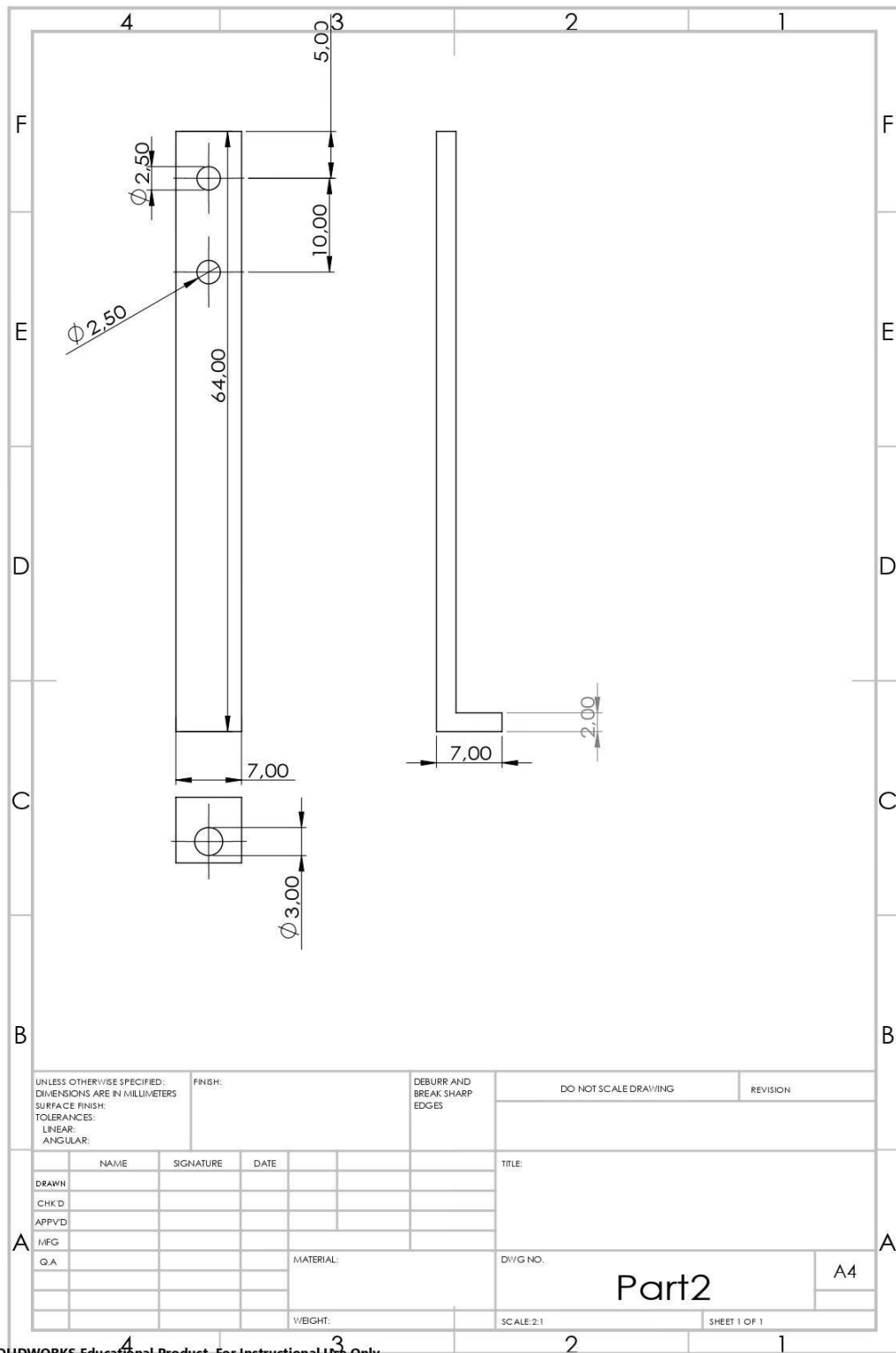


## 7.2.4 Isolating Piece



SOLIDWORKS Educational Product. For Instructional Use Only.

## 7.2.5 Connecting Rod



SOLIDWORKS Educational Product. For Instructional Use Only.